Postprint of: Nowosielski B., Jamrógiewicz M., Łuczak J., Tercjak A., Warmińska D., Effect of temperature and composition on physical properties of deep eutectic solvents based on 2-(methylamino)ethanol – measurement and prediction, JOURNAL OF MOLECULAR LIQUIDS Vol. 371 (2023), 121069, DOI: 10.1016/j.molliq.2022.121069

Effect of temperature and composition on physical properties of deep eutectic solvents based on 2-(methylamino)ethanol – measurement and prediction

Bartosz Nowosielski[a], Marzena Jamrógiewicz[b], Justyna Łuczak[c, d], Agnieszka Tercjak[e], Dorota Warmińska[a,*]

[a] Department of Physical Chemistry, Faculty of Chemistry, Gdańsk University of Technology, ul. Narutowicza 11/12, 80-233 Gdańsk, POLAND

[b] Department of Physical Chemistry, Faculty of Pharmacy, Medical University of Gdańsk, Al. Gen. Hallera 107, 80-416 Gdańsk, POLAND

[c] Department of Process Engineering and Chemical Technology, Faculty of Chemistry, Gdańsk University of Technology, ul. Narutowicza 11/12, 80-233 Gdańsk, POLAND

[d] Advanced Materials Center, Gdańsk University of Technology, ul. Narutowicza 11/12, 80–233 Gdańsk, POLAND[c] Department of Physical Chemistry, Faculty of Pharmacy, Medical University of Gdańsk, Al. Gen. Hallera 107, 80-416 Gdańsk, POLAND

[e] Group 'Materials + Technologies' (GMT), Department of Chemical and Environmental Engineering, Faculty of Engineering, University of the Basque Country (UPV/EHU), Pza Europa 1, 20018 Donostia-San Sebastian, Spain

[*]Corresponding author: Tel.:+48583471410; fax:+48583472694,
e-mail address: dorwarmi@ pg.edu.pl

Abstract

Novel deep eutectic solvents were synthesized using 2-(methylamino)ethanol as hydrogen bond donor with tetrabutylammonium bromide or tetrabutylammonium chloride or tetraethylammonium chloride as hydrogen bond acceptors. Mixtures were prepared at different molar ratios of 1:6, 1:8 and 1:10 salt to alkanolamine and then Fourier Transform Infrared Spectroscopy measurements were performed to confirm hydrogen bonds interactions between components. Moreover, thermal properties such as melting points and thermal stability of deep eutectic solvents were determined and described. Each of important physical properties, including densities, viscosities, refractive indices and sound velocities at the temperature range of 293.15 - 333.15 K and the pressure of 0.1MPa, were measured and discussed. The effect of hydrogen bond acceptor to hydrogen bond donor molar ratio, anion and length of alkyl chain for each synthesized salt according to their properties was evaluated. Additionally, the experimental values of each physicochemical parameter were compared with the predicted ones calculated using models recommended in the literature. The main aim of this work was to assess the suitability of existing mathematical models for predicting the physicochemical properties of novel alkanolamine-based DESs. Empirical correlations for approximating phase behaviour or flow properties for DES systems are used in many procedures for design materials used of carbon-dioxide capture purposes. The obtained results indicate that in the case of deep eutectic solvents based on 2-(methylamino)ethanol, in the absence of any experimental data, the best models for density prediction are the bonding group interaction contribution method and the group contribution model. For modelling of the refractive index it has been confirmed that a method based on the critical properties is the most satisfying. However, for the viscosity and speed of sound, the absolute average relative deviations for the methods based on critical properties exceed the measurement uncertainties found in practice. Therefore, they do not seem suitable for an accurate estimation of these properties for deep eutectic solvents based on 2-(methylamino)ethanol.

KEY WORDS: DES; 2-(methylamino)ethanol; tetraalkylammonium salts; thermal stability; physical properties; prediction models

1. Introduction

In recent years, deep eutectic solvents (DESs) have been proposed as promising green media that could replace conventional industrial solvents to reduce environmental pollution and improve process efficiency [1][2]. The reason for such great interest in these media is their excellent properties similar to ionic liquids (ILs), such as negligible vapor pressure, non-flammability and good dissolving capacity of many compounds [3]. Moreover, they have several advantages over conventional ILs in that they are biodegradable, non-toxic and relatively easy and economical to prepare [4]. DESs are easy to prepare in high purity, and consist of two or three components that can interact through hydrogen bonds and/or electrostatic interaction, thus forming an eutectic mixture [2]. DESs have been reported in many applications so far, such as metallurgy, catalysis, organic synthesis, liquid-liquid extraction and other separation processes [5][6][7][8]. These neoteric solvents have also been used for gas absorption, polymer synthesis, biomass processing and drug solubilisation [9][2][10] .

The evaluation of DESs as new generation of solvents for various practical applications requires sufficient knowledge of their thermal and physical properties. Thermal properties such as melting point and decomposition temperature help to establish the operating conditions of the process. Physical properties such as density, viscosity, speed of sound and refractive index provide information on molecular interactions in the liquid that are essential for industrial device design as well as process modelling. Therefore, at present, many studies focus not only on the application, but also on the structure and physicochemical properties of deep eutectic solvents. So far, there have been a few reviews on this topic [1][6][2][11]. At the same time, the interest of prediction of the physicochemical properties of deep eutectic solvents has been increased, as determining the DES characteristics by experiments at all temperatures is time consuming and costly. Some models are able to predict the physical properties of DESs only from their structural properties, allowing the rejection of deep eutectic solvents with adequate properties even before the synthesis step. The most common predictive techniques that have been the subject of recent research regarding the physical properties of DES are group/atomic contribution methods [12]. Until now, group contribution methods have been used mainly to predict the critical properties and the acentric coefficient of pure DESs [13] [14], [15]. In the literature, attempts to model also density, refractive index, heat capacities, speeds of sound and surface tensions of deep eutectic solvents using GC methods can be found [16][12][17][18].

In the last five years, the primary efforts have been devoted to the physicochemical characterization of DESs based on alkanolamines that have a much higher CO_2 absorption capacity than other deep eutectic solvents [19]. So far, only deep eutectic solvents with

monoethanolamine (MEA) diethanolamine (DEA), methyldiethanolamine (MDEA) and monopropanolamine (AP) have been studied [20][21][22][23]. Mjalli *et al.* reported the experimental values of density, viscosity, surface tension and refractive index for the MAE combined with choline chloride, tetabutylammonium bromide and methyltriphenylphosphium bromide [20]. Murshid *et al* presented the density, viscosity and refractive index for DESs based on DEA [21] and Adeyemi *et al.* determined the thermal stability and the physical properties such as density, viscosity, conductivity, surface tension and refractive index for MDEA based DESs containing choline chloride [22]. Our group published the values of density, viscosity, speed of sound and refractive index for AP based DESs [23] and this study is an extension of this work. Herein, a new series of DESs containing 2-(methylamino)ethanol (MAE) as hydrogen bond donor (HBD) and tetrabutylammonium bromide (TBAB) or tetrabutylammonium chloride (TBAC) or tetraethylammonium chloride (TEAC) as HBA were prepared and characterized by Fourier Transform Infrared spectroscopy (FTIR). Thermal properties of the synthesized DESs were determined using differential scanning calorimetry (DSC) and thermogravimetric analysis (TGA) techniques. Basic physical properties such as density, speed of sound, viscosity and refractive index were measured in a wide range of temperature (293.15 - 333.15 K). The influence of temperature, salt chain length and molar ratio of HBA to HBD has been analysed. The experimental values of physical properties have been compared with the predicted ones. Depending on the property, various methods described in the literature, including group contribution methods, were used to model it. The predictive ability of the applied methods for density, viscosity, sound velocity and the refractive index of MAE-based DESs has been discussed.

2. Materials and methods

2.1 Chemicals and DESs preparation

Table 1 presents the information about the chemicals used in this study, and Figure 1 shows their chemical structures. 2-(methylamino)ethanol, tetrabutylammonium bromide, tetrabutylammonium chloride and tetraethylammonium chloride were purchased from Sigma-Aldrich. Tetrabutylammonium chloride was purified by double crystallization from acetone by adding diethyl ether and the others chemicals were used as received from the producer. All salts were dried under reduced pressure before use, TBAB at 323 K for 48 h, TBAC and TEAC at 298.15 K for several days.

The nine DESs were prepared by combining three different tetraalkylammonium salts and 2-(methylamino)ethanol in the molar ratio of 1:6, 1:8 and 1:10 HBA to HBD. The molar ratio of 1:6 was the lowest at which a stable DES could be obtained. Additionally, depending on DES, the eutectic composition was in the range of 1:6-1:10 molar ratios, thus in order to include the effect of molar ratio on the physical properties of analysed DESs, all liquids were tested at the given ratios. This also allowed comparison of the effect of hydrogen bond acceptors on the properties of DES with the same molar ratios. The preparation was carried out by mass, using appropriate amounts of each DES component (Mettler Toledo with the precision of 0.00001 g), mixed at 353.15 K for 1h until a homogeneous liquid without any precipitate was formed. The obtained DESs, stable colourless liquids at room temperature, were kept in tight bottles to prevent any contamination from outside atmosphere that may affect the physical properties of DES. Before experiments, the water content in DESs was measured by the Karl - Fischer Method using a Mettler Toledo Volumetric Karl - Fischer titrator (V10S). Table 2 presents its values along with the molar mass of DESs, their abbreviations, and the molar ratio and mass fraction of DES components.

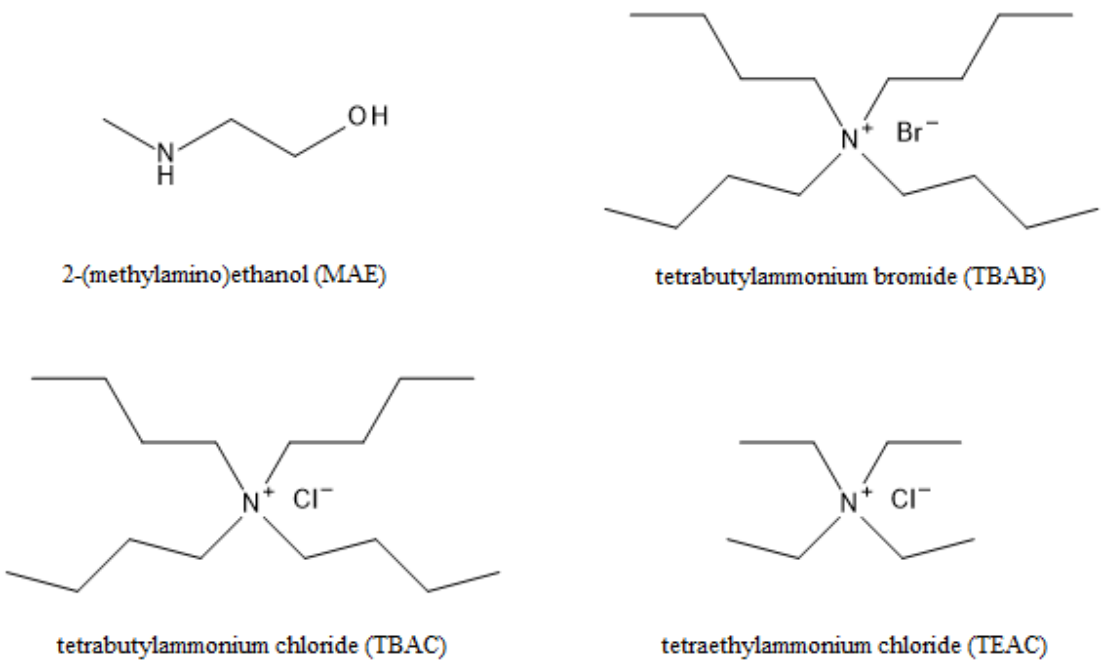

Figure 1 Chemical structures of the DESs components used in this study.

2.2 DES characterization

2.2.1. Infrared spectroscopy measurements

FTIR experiments for liquid samples were performed using Jasco-4700 instrument (4000–400 cm^{-1} with 32 scans, 4 cm^{-1} resolution; Jasco Company, Tokyo, Japan). Thin film method using salt (KBr) plates was applied by placing 1 drop of the solution on one salt plate. The spectrum from a clean plate was recorded as a background and analysis of spectra was performed using Spectra Analysis software (Jasco Company, Tokyo, Japan). Spectra of solid samples (substrates) were recorded using dry salt KBr. The materials (1 mg) were compressed with potassium bromide (99 mg) to form a disc. Analysis were performed at 298.15 ± 0.1 K.

Table 1 Provenance and mass fraction purity of the compounds studied.

Chemical name	Source	CAS number	Initial purity/ mass fraction[a]	Purification method	Final purity/ mass fraction[a]
2-(methylamino)ethanol (MAE)	Sigma Aldrich	109-83-1	≥0.98	none	-
Tetrabutylammonium bromide (TBAB)	Sigma Aldrich	1643-19-2	≥0.99	none	-
Tetraethylammonium chloride (TEAC)	Sigma Aldrich	56-34-8	≥0.98	none	-
Tetrabutylammonium chloride (TBAC)	Sigma Aldrich	1112-67-0	≥0.97	crystalization	≥0.98[b]

[a] As stated by the supplier
[b] Determined by potentiometric titration

2.2.2 Melting point

Mettler Toledo Star One Differential Scanning Calorimeter (DSC) was used to measure the melting points of the synthesized DESs. The measurements were made under purified nitrogen atmosphere with a flow rate of 60 $mL \cdot min^{-1}$, with samples of 10 – 18 mg packed in standard aluminium pan. The DSC equipment was connected to the STAR® data acquisition software a dedicated computer. The heating and cooling sequence was programmed on the STAR® console which controls the DSC equipment. For the melting point determination, a temperature range from 193.15 to 298.15 K was selected with a heating rate of 2 $K \cdot min^{-1}$. The uncertainty of the measurement was ± 0.01 K.

2.2.3 Thermogravimetric analysis

The thermogravimetric analysis were performed using the TG 209F3 apparatus from Netzsch Group (Selb, Germany). Weighted samples (approx. 10 mg) were placed in a corundum dish. The measurement was carried out in an inert gas atmosphere-nitrogen with a flow rate of 50 $ml \cdot min^{-1}$ at the temperature range from 298 to 1023 K at a heating rate of 10 $K \cdot min^{-1}$.

2.2.4 Density and sound velocity

The densities and the sound velocities of the DES samples were obtained at different temperatures using a digital vibration-tube analyser (Anton Paar DSA 5000, Austria) with proportional temperature control that kept the samples at working temperature with an accuracy of ±0.01 K. Experimental frequency for the measurements of the ultrasonic velocity was equal to 3 MHz. The calibration was carried out using double distilled, deionized and degassed water, and dry air at atmospheric pressure (0.1 MPa). The standard uncertainty of density measurement was better than 0.1 $kg \cdot m^{-3}$ and 0.5 $m \cdot s^{-1}$, respectively.

2.2.5 Viscosity

The viscosities of the DESs were measured with a LVDV-III Programmable Rheometer (cone-plate viscometer; Brookfield Engineering Laboratory, USA), controlled by a computer. The temperature of the samples was controlled within ± 0.01K using a thermostatic water bath (PolyScience 9106, USA). The display of the viscosimeter was verified with certified viscosity standard N100 and S3 provided by Cannon at 298.15 ± 0.01 K. The standard uncertainty of viscosity measurement was better than 2%. At least three independent measurements were taken for each sample at each temperature to assure reproducibility of the measurement.

2.2.6 Refractive index

The refractive indices were obtained with an Abbe refractometer (RL-3, Poland) equipped with a thermostat for controlling the cell temperature with an accuracy of ± 0.1 K. The standard uncertainty of refractive index measurement on the n_D scale was 0.0002. At least three independent measurements were taken for each sample at each temperature to assure reproducibility of the measurement.

Table 2 The abbreviation, molar mass, molar ratio, mass fraction and water content for chemicals used in this work.

DES		Salt		HBD		Molar ratio		Mass fraction[a]		Water content[b]
Symbol	M_{DES} / ($g \cdot mol^{-1}$)	Abbreviation	M_{salt} / ($g \cdot mol^{-1}$)	Abbreviation	M_{HBD} / ($g \cdot mol^{-1}$)	Salt	HBD	Salt	HBD	
DES1	110.601	TBAB	322.37	MAE	75.11	1	6	0.4183	0.5817	0.0015
DES2	102.072	TBAB	322.37	MAE	75.11	1	8	0.3444	0.6556	0.0018
DES3	97.675	TBAB	322.37	MAE	75.11	1	10	0.3012	0.6988	0.0020
DES4	87.915	TEAC	210.16	MAE	75.11	1	6	0.2664	0.7336	0.0017
DES5	85.206	TEAC	210.16	MAE	75.11	1	8	0.02167	0.7833	0.0018
DES6	83.390	TEAC	210.16	MAE	75.11	1	10	0.1816	0.8184	0.0021
DES7	104.336	TBAC	277.92	MAE	75.11	1	6	0.3838	0.6162	0.0020
DES8	97.629	TBAC	277.92	MAE	75.11	1	8	0.3161	0.6839	0.0025
DES9	93.574	TBAC	277.92	MAE	75.11	1	10	0.2704	0.7296	0.0028

[a] The standard uncertainty of DES mass fraction composition is 0.001

[b] Water content of DESs in mass fraction determined by Karl Fisher titration with the standard uncertainty ±0.0001.

2.3 Prediction methods of DESs physical properties

2.3.1 Density modelling

Prediction of the MAE-based DESs density was performed by seven different methods described below. The two firstly applied models, Spencer – Danner procedure [25] and Mjalli *et al.* method [26], are based on the Rackett equation [24]. Generally, both models require the knowledge of the critical parameters such as the temperature, the volume and the pressure of DESs. Since these properties of DES components cannot be conveniently found experimentally, the Modified Lydersen-Joback-Reid method [27] proposed by Alvarez and Valderrama seems to be an important facilitation. The authors used Joback−Reid equations for the normal boiling temperature and the critical temperature. Additionally, Lynders equations for the critical pressure and critical volume were improved by their own modifications in parameters involved in equations. It resulted in new method which gives good results for different molecules with high molecular mass. Apart of that the critical properties of novel DES are found using the Lee-Kesler mixing equations suggested by Knapp *et al.* [28].

Prediction of DES density based on the modified Rackett equation was employed as follows:

$$d = d_R / Z_{RA}^{\varphi} \tag{1}$$

where parameter φ is defined as :

$$\varphi = (1 - T/T_{cm})^a - (1 - T_R/T_{cm})^a \tag{2}$$

and Z_{RA} is the specific compressibility factor can be calculated using:

$$Z_{RA} = \left(\frac{V_{RS} P_{cm}}{R T_{cm}}\right)^b \tag{3}$$

In equations 1-3, the symbols: d_R, T_R, and V_{RS} represent the reference density, reference temperature and saturated molar volume at reference temperature, respectively. The constants a and b are equal to 2/7 and $\left(1/[1 + (1 - T/T_{cm})^{2/7}]\right)$ for the modification of Spencer and Danner, while for the model proposed by Mjalli *et al.* are equal to 16/7 and $\left([5/24 + T_R/T_{cm}]^{16/7}\right)$.

Going further, the density of the MAE-based DESs was predicted by the investigation performed by model introduced by Haghbakhsh *et al.* [29]. The authors used density as a databank for 149 DESs at several temperatures and a genetic programming algorithm to derive a DES density prediction model that uses the critical temperature, critical volume and acentric factor. Finally, they obtained the equation:

$$d = A_1 T_{cm}^2 + A_2 T_{cm} + A_3 \omega^{0.2211} + A_4 V_{cm} + BT \quad (4)$$

where $A_{1\text{-}4}$ and B are the model's parameters presented in Table S1.

Another method of predicting the DESs densities was the bonding-group interaction contribution method introduced by Hou *et al.* [30]. Here, each group and bounding group interaction (BGI) make its own contribution to the density of the DES components.

Thus, the density can be predicted by following equation:

$$1/d = \frac{w_1}{(A_1+B_1T)\sum_j n_{1j}\Delta d_{1j}+A_2+B_2T} + \frac{w_2}{(A_1+B_1T)\sum_j n_{2j}\Delta d_{2j}+A_2+B_2T} + ww_2TG_{III} \quad (5)$$

where w_1 and w_2 are the mass fractions of DES components, Δd_{1j} and Δd_{2j} are the contribution values of the corresponding group j for density of DES components, A_1, A_2, B_1, and B_2 are the model's constants and G_{III} is the constant that represents interactions in type III deep eutectic solvents.

Each parameters involved in presented models are presented in Table S2. For MAE-based DESs investigated in this work, only one bounding group interaction, i.e. (OH-NH) in 2-(methylamino)ethanol molecule should be considered and the values of $\sum_j n_j d_j$ for TBAB, TEAC, TBAC and MAE are 0.0497; 0.0407; 0.0186 and 0.0252 respectively.

Lastly, the method by Mjalli [31] was applied for prediction of the DESs densities. It is a model based on the mass connectivity index with the semi-empirical equation as follows:

$$d = d_R - 0.0005197\lambda_{DES}^{0.18293}(T - T_R) \quad (6)$$

where λ_{DES} is the mass connectivity index of DES, calculated on the basis of the pure components mass connectivity indices λ, which are obtained from equation:

$$\lambda = \sum_{k=1}^{ij}\left(1/\sqrt{M_i M_j}\right) \quad (7)$$

where M_i and M_j are the masses of connected groups numbers (i) and (j) reported by Vaderrama *et al.* [32].

In this work, the mass connectivity indices for 2-(methylamino)ethanol, tetrabutylammonium bromide, tetraethyl-ammonium chloride and tetrabutylammonium chloride are obtained as 0.5428, 2.3215, 1.5617 and 2.3515, respectively. Correlation with ones calculated by multiplying the salt and MAE mass connectivity indices by their molar quantities in the DES is presented in Table 6.

Other known and applied models for predicting densities, refractive indices, heat capacities, speeds of sound, and surface tensions of novel DESs presented in this work are methods described by Haghbakhsh *et al.* in 2021 [12]. This is *a* group contribution (GC) and atomic contribution (AC) density models which use a 1239 point dataset.

The GC based method is expressed as:

$$d_1^G = m_{HBA} \sum k_i \left(\Delta d_{1,i}^G\right)_{HBA} + m_{HBD} \sum l_j \left(\Delta d_{1,i}^G\right)_{HBD} \quad (8)$$

$$d_2^G = m_{HBA} \sum k_i \left(\Delta d_{2,i}^G\right)_{HBA} + m_{HBD} \sum l_j \left(\Delta d_{2,i}^G\right)_{HBD} \quad (9)$$

$$d^G = \left(\frac{d_i^G}{M_w}\right)^{-0.2045} + \left(\frac{d_2^G}{M_w}\right) T^{-0.6785} + 1.3695 \quad (10)$$

while AC model is as follows:

$$d_1^A = m_{HBA} \sum k_i \left(\Delta d_{1,i}^A\right)_{HBA} + m_{HBD} \sum l_j \left(\Delta d_{1,i}^A\right)_{HBD} \quad (11)$$

$$d_2^A = m_{HBA} \sum k_i \left(\Delta d_{2,i}^A\right)_{HBA} + m_{HBD} \sum l_j \left(\Delta d_{2,i}^A\right)_{HBD} \quad (12)$$

$$d^A = \left(\frac{d_1^A}{M_w}\right)^{-0.4093} + \left(\frac{d_2^A}{M_w}\right) T^{-0.7434} + 0.5139 \quad (13)$$

where M_w is the molar mass of DES and $\Delta d_{1,i}$, $\Delta d_{2,i}$, are the contributions of each group/atom of type i for the GC and AC models. k_i and l_j indicate the number of occurrence of the functional group/atom of type i in the HBA and HBD molecules, respectively. The symbols m_{HBA} and m_{HBD} denote the normalized numbers of moles HBA or HBD. In this study, there was no need for data normalization as the number of mols of the hydrogen bond donor expressed per one mole of hydrogen bond acceptor. The G and A superscripts show the GC and AC model type, respectively.

2.3.2 Prediction of viscosity

The viscosity of deep eutectic solvents prediction was estimated by model proposed and described by Bakhtyari *et al.* [33]. Basing on a databank of 156 DESs and 1308 data points and the knowledge of the critical pressure, critical temperature, and one reference viscosity data, they developed an useful model expressed as:

$$\eta = \left[\eta_R^A + B\left(\frac{T_R - T}{T \cdot T_R}\right)\right]^{1/A} \quad (14)$$

where the constant A is related to the critical pressure, P_{cm}:

$$A = \frac{-0.817}{P_{cm}} - 0.123 \quad (15)$$

and the constant B depend on the critical temperature, T_{cm} as:

$$B = -1.595 T_{cm} \quad (16)$$

In equation 14, the symbol η_R denotes to the viscosity at the reference temperature T_R.

For the DESs investigated in this study, the reference temperature is 293.15 K.

2.3.3 Prediction of refractive index

Four different methods were used to predict the MAE-based DESs refractive index in this work. Firstly, we applied model developed by Shahbaz *et al.* [13] and the authors applied here the molar refractions (R_M) of DESs components calculated by summing their atomic and structural contribution parameters that were determined by Wildman and Crippen [34]. The molar refraction of DESs was obtained from the equation:

$$R_M = \sum x_i R_{Mi} \tag{17}$$

where x_i and R_{Mi} are the mole fraction and molar refraction of the DES components, and its value together with the experimental value of DES density was used to calculate the refractive index by Lorentz–Lorenz equation:

$$R_M = \frac{M_w}{d}\left(\frac{n^2-1}{n^2+2}\right) \tag{18}$$

where M_w and d are the molecular weight and density of DES, respectively.

While prediction of refractive index for the components of novel DESs used in this study, the molar refractions (R_M) were found to be equal to 21.012, 87.567, 47.557 and 84.493 for MAE, TBAB, TEAC and TBAC, respectively.

The second method that we tested on the ability to predict the DESs refractive index was based on the critical properties and acentric factors developed by Taherzadeh *et al.* [35]. In the model the following equation was proposed:

$$n = A_1\omega^3 + A_2\frac{\omega^2}{M_w} + A_3P_{cm} + A_4 + B\omega/T \tag{19}$$

where A_1-A_4 and B are parameters of model presented in Table S3.

Going further, prediction of the refractive index for novel chloride and bromide-based deep eutectic solvents was performed by the group contribution model introduced by Khajeh *et al.* [18]. Unfortunately, this method does not include bromide-based deep eutectic solvents that have an amine group contained in hydrogen bond donor, therefore, in this work, the model by Khajeh *et al.* could be used to predict only the refractive indices of TEAC:MAE and TBAC:MAE. The model proposed by authors was as follows:

$$n = \sum N_i GC_i + 0.22766\,HBA/HBD - 0.00037T + 1.37466 \tag{20}$$

where N_i and GC_i are the number of occurrences of ith chemical substructure (functional group) and the contribution of the ith chemical substructure, respectively, T is temperature in K and HBA/HBD is molar ratio of HBA to HBD.

Lastly, we used the method described by Haghbakhsh *et al.* [12]. It is modeled on group contribution and atomic contribution and uses a large dataset of 1117 data points from 142 DESs. The GC model was expressed as:

$$n^G = \left(n_i^G\right)^{-0.3597} + (n_2^G)T^{-1.8254} + 1.3695 \quad (21)$$

while AC model was as follows:

$$n^A = (n_1^A M_w)^{-0.2975} + (n_2^A M_w)T^{-2.9213} + 1.4335 \quad (22)$$

In this work, the refractive indices of the pure components were calculated using the equations analogous to Equations 8 and 9 using the contribution of each group/atom.

2.3.4 Prediction of speed of sound

Generally, three methods were described to estimate the speed of sound of DESs, while two of them were applied in this study. The first model was proposed by Peyrovedin *et al.* [16] and required knowledge of the critical parameters of solvent. It was expressed as:

$$u = \omega(7.378M_w - 2.012T) - 2.911V_{cm} + 2514.2 \quad (23)$$

The next two were based on atomic and group contribution and were introduced on the basis 398 data points by Haghbakhsh *et al.* [12]. Unfortunately, due to the lack of NH group contribution data, the GC based model could not be used to predict the speed of sound of MAE-based DESs studied in this work. Moreover, as there is no data on the atomic contribution of the bromide ion, it was also impossible to model of the speed of sound for TBAB based DESs (DES1-DES3).

The AC based model was expressed as:

$$u^A = u_1^A + u_2^A T^{0.0258} + 1607.4690 \quad (24)$$

where the speed of sound for the pure components were calculated using the equations analogous to Equations 11 and 12 using the atomic contribution of each atom.

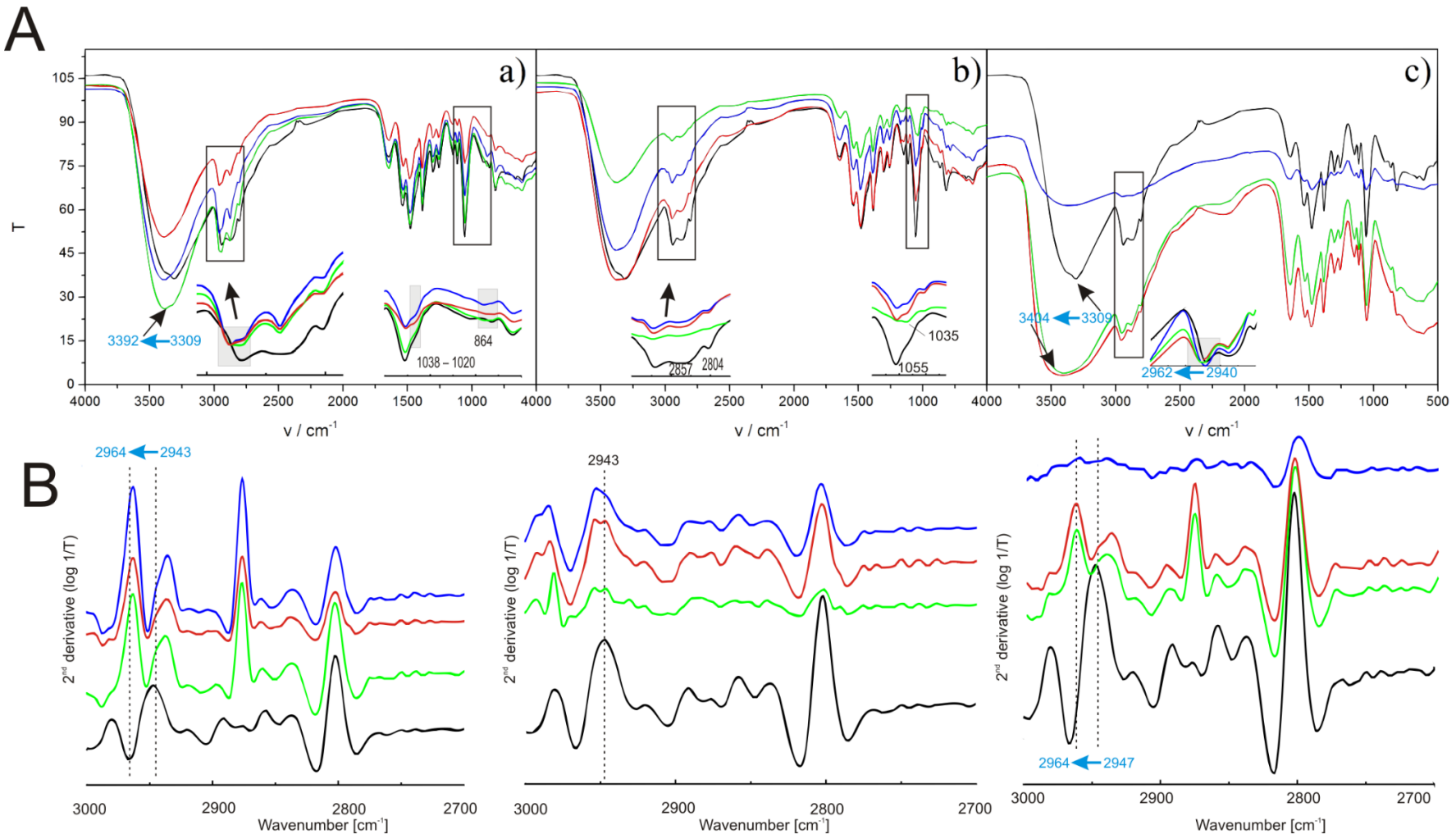

Figure 2 A FTIR spectra and B their second derivatives for DES studied: a) TBAB:MAE (DES 1-3) , b) TEAC:MAE (DES 4-6) and c) TBAC:MAE (DES 7-9); (blue – 1:6, red – 1:8, green – 1:10; black – neat MAE).

3. Results and discussion

3.1 FTIR characterization of DESs

Infrared spectroscopy may be used not only as standard method for identification of molecular vibrations and deformations of chemical bonds in DES, but also as a means of individual characteristic interactions of a similar chemical structures [20][36]. The FTIR spectra of the studied DESs are shown in Figure 2 together with the reference of neat 2-(methylamino)ethanol spectrum (black line at Figure 2).

The bands in the MAE spectrum present typical region of the ν(OH)/ν(NH_2) stretching vibrations range (3000–3900 cm^{-1}), particularly sensitive to the hydrogen bonding located at 3309 cm^{-1}. The DES spectra presented maximum absorption of these interactions at 3392 cm^{-1} with TBAB salts (DES 1–3), 3378 cm^{-1} with TEAC (DES 4–6) and 3404 cm^{-1} with TBAC (DES 7-9) so there are blue-shifted effects observed which mean the increase of energy. The observed frequency and intensity variations follow naturally. Interestingly, in the spectrum of TBAB:MAE the C−H stretching vibrations of the CH_2−CH_2 backbone in MEA were blue-shifted from 2943 to 2964 and from 2857 to 2873 cm^{-1}, respectively for DES 1–3. On the second derivatives of TBAC:MAE spectra blue-shifts of band 2964 ← 2947 cm^{-1} are observed. In the studied DESs, the other spectroscopic effect on the spectra are observed at the range1100-1000 cm^{-1}. The stoichiometry and amount of salt influence is visible as the change of band shape. In TBAB:MAE spectrum flattening at 1038 - 1020 cm^{-1} for C-N stretching amine of the 1:10 stoichiometry sample (green) is more noticeable than for the 1:6 and 1:8 samples because it corresponds to the shape of the MAE band (Fig. 2 a). In the sample containing 1:10 stoichiometry of TEAC:MAE spectrum at 1055 cm^{-1} is influenced and become deformed to more intensive one at 1035 cm^{-1} (Fig. 2 b). DES with TBAC seems as the same at this region. Substituted C-H bending at 864 cm^{-1} of each DESs spectrum is not interrupted.

3.2. Thermal properties of DESs

The obtained thermal properties of the studied DESs based on 2-(methylamino)-ethanol are shown in Table 3, as the values of melting temperature, T_m , decomposition temperatures at 10% and 90% weight loss, $T_{10\%}$ and $T_{90\%}$, and maximum temperatures, T_{max}. Figure 3 presents the DSC plots and Figure 4 shows the curves TGA with DTGA.

3.2.1. Melting point

Differential scanning calorimetry is crucial for observing the phase transition temperature of materials. DSC has been used to determine the melting point and any solid state phase transitions in the present of MAE-based DESs. Table 3 shows the melting points of DESs. Fig. 3 (a,b,c) illustrates DSC curves for the DES systems with three HDA:HBD ratios as 1:6; 1:8 and 1:10. Generally, in most curves there are doublet form endothermic peaks which are considered as melting peaks, but in the case of TBAB:MAE 1:6 we observed a single peak of melting process. For the studied DESs all the melting points were lower than for the pure components and below 255.15 K which gives them wide liquid range. Clear crystallization and melting peaks were observed for all tested DESs. Moreover, the order of melting temperatures for DES at the same molar ratio of the salt to 2-methylaminethanol is as follows: TBAB:MAE > TEAC:MAE > TBAC:MAE, which seems to suggest that the melting temperature of salt may influence the melting temperature of deep eutectic solvents. Besides, the highest values of T_m are observed for tetrabutylammonium bromide based DESs, which T_m is greater than that of TBAC. Moreover, the comparison of the melting temperatures for DES containing tetrabutylammonium and tetraethylammonium chlorides leads to the conclusion, that the melting temperature of deep eutectic solvents increases with increasing cation alkyl chain length in the salt and T_m of salt itself. The same results were obtained for DESs with 3-amino-1-propanol [23]. DSC thermograms are shown in Figure 3. Additionally, it has been observed that the phase transition temperatures only for TBAB 1:8 and 1:10 are present at temperature near 250.15 K. All determined results are given in Table 3.

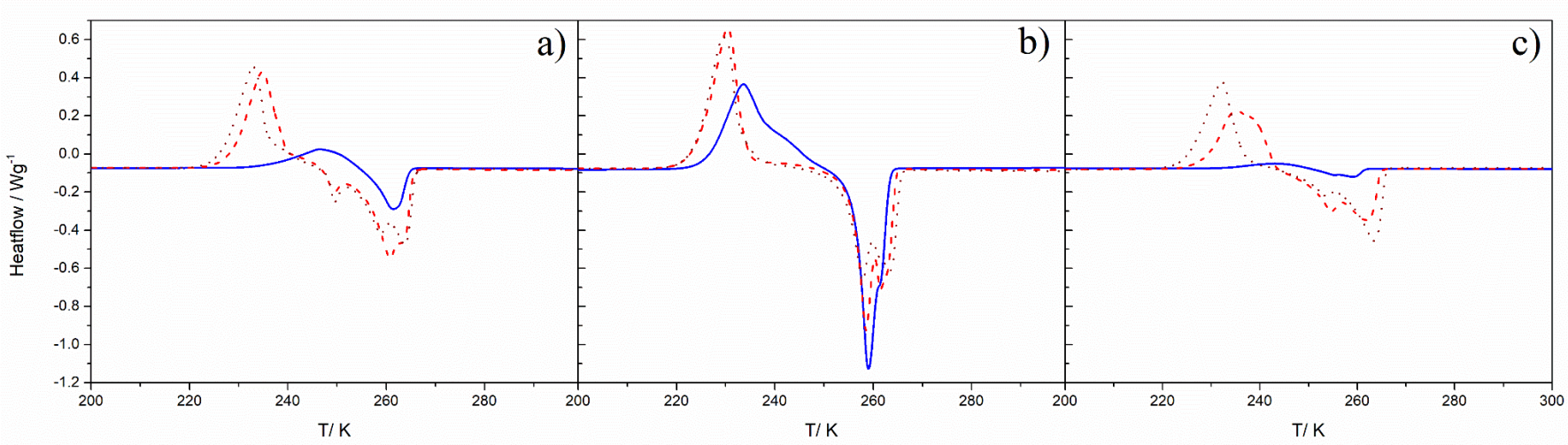

Figure 3 DSC curves for DES studied: a) TBAB:MAE (DES 1-3) , b) TEAC:MAE (DES 4-6) and c) TBAC:MAE (DES 7-9); (blue solid line – 1:6, red dashed line – 1:8, wine dotted line– 1:10).

3.2.2. Thermogravimetric measurements

Figure 4 presents TGA curves, *i.e*. the weight loss measured in % against temperature, for the studied DESs along with their pure components. In general, the curves consist of two steps– the first shows the MAE decomposition and the second corresponds to the degradation of the salt. Only for TEAC: MAE with the molar ratio of HBA to HBD of 1:10 at the lower temperature (approx. 373K) an additional step is observed. The reason of this observation may be explained by evaporation of water. As the water content of all primary samples (see Table2) was very similar, hence the higher amount of water in TEAC: MAE (1:10) shown in the TGA curve could to be the result of moisture absorption from the atmosphere when this DES was transferred to the TGA pan.

As can be seen from the TGA plots, the stability of all DESs is in between that of their components and the order of stability is: MAE < DES < salt.

For DESs with a molar ratio of HBA to HBD equal to 1:6 and 1:10, the initial decomposition temperature measured as 10% weight loss ($T_{10\%}$) and the first significant peak of derivative weight loss curve (T_{max1}) change according to the sequence: TBAB:MAE < TEAC:MAE < TBAC:MAE, while for DESs with the molar ratio 1:8, the order of $T_{10\%}$ is different, as is TEAC:MAE < TBAB:MAE < TBAC:MAE (Table 3). Indication of the end of the decomposition is measuring 90% mass loss ($T_{90\%}$) and the second significant peak of derivative weight loss curve (T_{max2}). Results approved that they change regardless of the molar ratio of HBA to HBD according to: TBAB:MAE < TBAC:MAE < TEAC:MAE (Table 3). Thus, it can be concluded, that when DESs with the same molar ratio are considered, the highest thermal stability, measured by $T_{10\%}$ and $T_{max1,}$ is found for TBAC:MAE, which is more stable than TEAC:MAE. Moreover, since the decomposition temperature observed for TBAB:MAE is lower than for TBAC:MAE, it can be claimed that DESs based on salts containing a chloride anion are more stable than those containing a bromide anion. Obviously, this correlates with the strength of the hydrogen bonds, which is stronger for the Cl^- than for Br^- and this effect seems to be stronger than the effect of the alkyl chain length in the salt because the decomposition temperature of TBAB:MAE is lower than that of TEAC:MAE. The exceptions to this rule are DESs with a molar ratio 1:8, for which an inverse $T_{10\%}$ correlation for TEAC:MAE and TBAB:MAE is observed. As the molar ratio 1:8 is the eutectic composition for TBAB:MAE (Table 3), the stronger hydrogen bonds are expected in this solvent and make it more stable. The positive effect of the eutectic composition on the thermal stability of DESs is also seen in DESs based on the same salt but differing in the molar ratio of HBA to HBD

(see Figure 4). Summing up, it can be said that our conclusions are consistent with the results obtained for phosphonium-based DES, showing that the thermal stability of DES increases with increasing length of the alkyl chain length of its components and is higher for systems with stronger hydrogen bonds interactions [37].

Table 3 Thermal characteristics obtained from TGA, DTGA and DSC curves: decomposition temperatures at 10% and 90% weight loss, $T_{10\%}$ and $T_{90\%}$, maximum temperatures, T_{max}, melting temperature, T_m , heat of crystallization, ΔH_{cryst} , heat of melting, ΔH_m, and heat of other solid transitions for DESs in this work.

DES	$T_{10\%}$ / K	$T_{90\%}$ / K	T_{max1} / K	T_{max2} / K	T_m / K	$\Delta H_{cryst.}$ $(mJ K^{-1})$	ΔH_m $(mJ K^{-1})$	ΔH_{other} $(mJ K^{-1})$
DES1	333.9	494.0	361.7	489.6	261.28	-	262	-
DES2	356.8	494.4	383.6	489.7	260.75	235	262, 264	250
DES3	332.2	489.9	360.6	489.5	263.83	232	259, 264	250
DES4	341.1	546.6	367.6	547.6	258.99	234	259, 262	-
DES5	340.6	543.0	368.1	548.2	258.62	235	259, 262	-
DES6	339.5	547.7	389.0	554.2	258.03	231	258, 264	-
DES7	376.8	506.1	409.8	497.9	259.02	-	255, 259	-
DES8	373.4	503.7	407.4	498.2	261.37	241	262, 255	-
DES9	367.0	490.5	404.0	486.9	263.43	233	254, 264	-
MAE	329.1	379.1	368.5	-	268.25	-	-	-

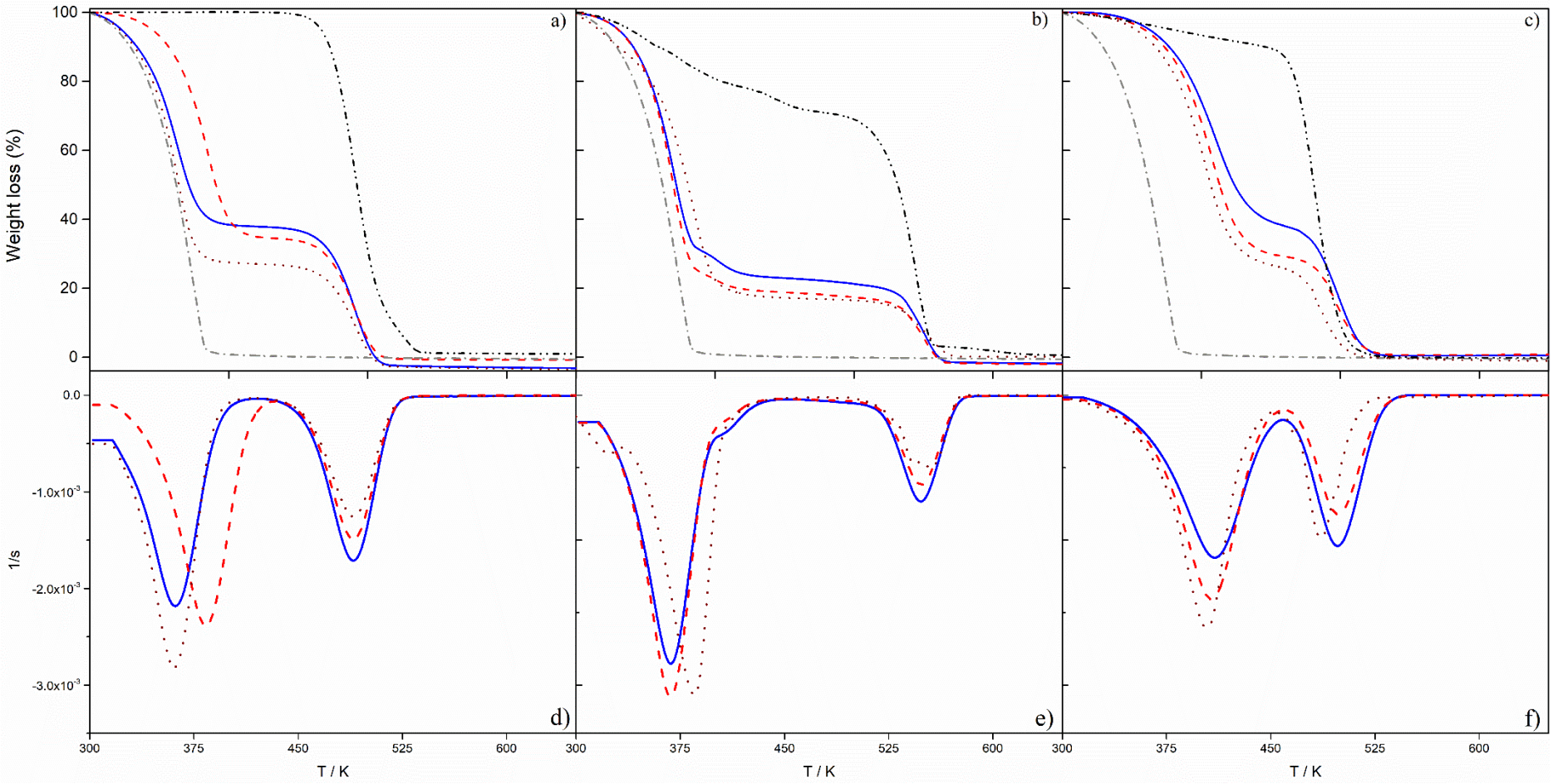

Figure 4 TGA curves: (a, b, c) and DTGA curves: (d, e, f) obtained by thermogravimetry of DESs: a) and d) TBAB:MAE (DES 1-3) , b) and e) TEAC:MAE (DES 4-6); c) and f) TBAC:MAE (DES 7-9); (blue solid line – 1:6, red dashed line – 1:8, wine dotted line – 1:10, black dash-dotted-dotted line – salt, grey dashed-dotted line – MAE).

3.3. Experimental values of physical properties of DESs

3.3.1 Density

In this study, the density and other physical properties of the deep eutectic solvents studied were measured as a function of temperature with the range of 293.15 - 333.15 K and at ambient pressure. All density data are presented in Table S4. Figure 5 depicts, as example, the obtained densities for TBAB:MAE, TEAC:MAE and TBAB:MAE at a molar ratio of 1:8.

As can be seen from Table S4, the experimental density values decrease with increasing temperature and the decrease is linear, as shown in Figure 5. This is obviously due to the fact that at higher temperatures, more intermolecular voids are created, which increase in volume and lead to a decrease in density.

Moreover, the values of the DESs density at the same temperature and molar ratio of the salt to 2-(methylamino)ethanol are highest for TBAB based DESs and lowest when TBAC plays the role of HBA. The same order of density was found by our group for 3-amine-1-propanol based DESs consisting of the same salts, i.e. TBAB:AP > TEAC:AP > TBAC:AP [23]. The Smith and Zhang groups also postulated that bromide salts lead to denser DESs than chlorides [38][2].

The results obtained for TBAC:MAE and TEAC:MAE are also consistent with reports in the literature showing that the density of DESs decreases with increasing of chain length of HBD or HBA. Florindo *et al.* showed that the DESs composed of glutaric acid and levulinic acid have lower density values compared to those observed for DES based on oxalic or glycolic acids [39]. Wang *et al.* reported that the density of ethylene glycol based DESs consisting of tetraethylammonium bromide, tetrapropylammonium bromide and tetrabutylammonium bromide were 1.1596, 1.1121 and 1.0762 at 298K, respectively [40].

As the density values for TBAB:MAE (DES 1-3) are higher than those for TEAC:MAE (DES 4-6) it can concluded that the packaging effects have a smaller influence on the density than the anion weight effect (anion charge density resulting from its size).

Further inspection of results presented in Table S4 and Figure 5 allow to claim that the DESs density depends on the HBA:HBD molar ratio. For deep eutectic solvents based on TBAB and TEAC, the density decreases as the content of MAE increases, while for TBAC-based DESs the effect of the molar ratio of HBD is negligible. It is well known that the influence of the amount of hydrogen bond donor on the density of DES depends on the molecular characteristics of HBD [20][41]. For most DESs, their density decreases as the amount of HBD increases. However, in the case of DES, where there is a strong association between HBD

molecules, an increase in density with the increase in the content of hydrogen bond donor was observed. Abbott *et al.* reported densities of DESs with different molar ratios of choline chloride to glycerol and found that the as the amount of HBD increased relative to the salt, the density increased [42]. In the case of the DES analyzed in this study, a different relationship between the density of deep eutectic solvents and the molar ratio of HBA to HBD seems to be related to the density of neat MAE. The densities of TBAB:MAE (DES 1-3) and TEAC:MAE (DES 4-6) are higher than those of 2-(methylamino)ethanol, while the densities of TBAC:MAE (DES 7-9) are almost the same, especially at lower temperatures. Thus, when the amount of 2-(methylamino)ethanol in TBAB:MAE (DES 1-3) and TEAC:MAE (DES 4-6) increases, the density tends to that of MAE and decreases. In the case of TBAC:MAE (DES 7-9), due to similar density of DES and neat MAE, no significant changes in density are observed as a result of changing the DES composition.

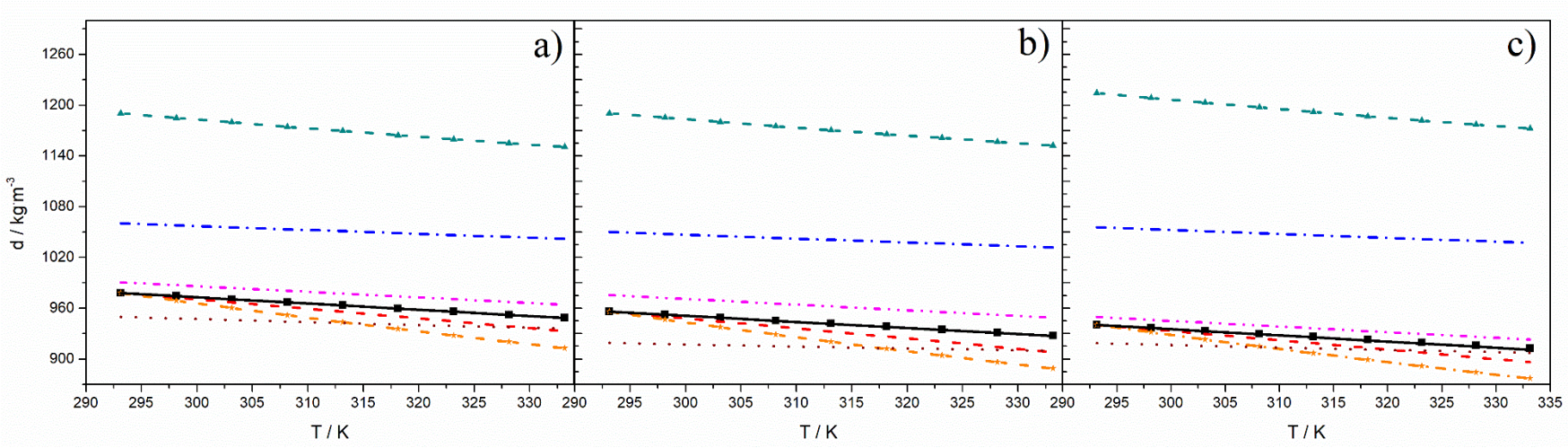

Figure 5 Experimental values of densities (black squares) for DESs in the molar ratio 1:8 along with the predicted ones a) TBAB:MAE, b) TEAC:MAE, c) TBAC:MAE: red dashed line – method based on Rackett equation by Spencer and Danner; orange dashed line with stars – method based on Rackett equation by Mjalli; blue dashed-dotted line – method based on critical properties by Haghbakhsh *et al.;* magenta dash-dotted-dotted line – BGI based method by Hou *et al.;* black solid line – MCI based method by Mjalli; wine dotted line – GC based method by Haghbakhsh *et al.;* dark cyan dashed line with triangles – AC based method by Haghbakhsh *et al.*.

3.3.2 Viscosity

The viscosity values of MAE-based DESs are in the range of 17.43÷34.27 mPa·s at 298.15 K (see Table S5) and therefore are among the lowest of recorded so far for DESs containing ethylene glycol, ethanolamine or acetic acid [43]. Moreover, as in the case of other deep eutectic solvents, the viscosity of TBAB:MAE, TEAC:MAE and TBAC:MAE decreases greatly with increasing temperature [44], [45]. According to the hole theory, as the viscosity is related to the free volume and the probability of finding holes of suitable dimensions into which solvent molecules or ions can move, this property depends on the size of the DES constituents [46]. The value of viscosity of DESs is also a result of the presence of hydrogen bonds, electrostatic and van der Waals interactions between the individual components of DESs. Thus, the viscosity depends on the chemical nature of the components, their molar ratio, water content and temperature [47]. As shown in Table S5 and Figure 6, the lowest viscosity values for the studied systems were observed for TEAC-based DESs (DES4-6), which are smaller in size and where weaker hydrogen bonding is expected, thus this is consistent with the hole theory [46][48]. Additionally, the shorter alkyl chains in TEAC might result in weaker van der Walls interaction.

It is also observed that the values of viscosities obtained both for TBAB:MAE (DES1-3) and TBAC:MAE (DES7-9) are similar. Therefore, it can be claimed that for deep eutectic solvents consisting of MAE and tetraalkylammonium salts, the alkyl chain length of the salt has a greater influence on the viscosity than the anion effect.

Regardless of the salt, the viscosity of MAE-based DESs decreases as the molar ratio of HBA to HBD increases. This is due to the low molecular movement caused by the decrease in the free volume of the solvent with the compact structure of DES [49]. Similar observations that increasing the amount of HBD reduces the viscosity of DES were made by most of the authors [39][50][41]. However, it should be noted, that in the case of DESs based on hydrogen bond donors with a strong cohesive energy due to presence of intermolecular hydrogen bond network, the opposite effect was also observed. At the temperature of 298 K, the viscosities of the mixtures of choline chloride and glycerol in a molar ratio of 1:4, 1:3, 1:2 are 350, 320, and 259 mPa·s, were found, respectively [42].

Analyzing results presented in Figure 6, it is noticed that viscosities for TBAB:MAE, TEAC:MAE and TBAC:MAE at a molar ratio of 1:8 of DESs evaluated in this work decreases nonlinearly with increasing temperature. Obviously, this is due to a significant decrease in hydrogen interactions with the temperature rising and increasing of the DES component

mobility. There are two commonly used models to study the effect of temperature on DESs viscosity, namely the Arrhenius and Vogel-Fulcher-Tamman (VFT) equations [51]. The Arrhenius (1) and VFT equations (2) are expressed as:

$$\eta = \eta_{\infty} exp(E_a/RT) \tag{25}$$

$$\eta = \eta_0 exp[b/(T - T_o)] \tag{26}$$

where η_{∞}, E_a, η_0, b, and T_o are fitting parameters, η_{∞} is the viscosity at infinite temperature, E_a is the activation energy, R is the gas constant, and T is the temperature at Kelvin.

Tables 4 and 5 present the fitting parameters determined from the experimental data along with R^2 and root-mean-square deviations (*RMSD*). The obtained E_a values, which are the lowest for TEAC:MAE and similar for TBAB:MAE and TBAC:MAE, confirm the conclusions presented above, *i.e.* the higher size of the DES components and the stronger interactions between them, the higher viscosity.

Comparing R^2 and *RMSD* values from Table 4 and 5 suggests the VFT equation is more suitable for fitting the dynamic viscosity results. Similar conclusions were made by for other alcoholamine-based DES, i.e. monopropanolamine-based deep eutectic solvents [23].

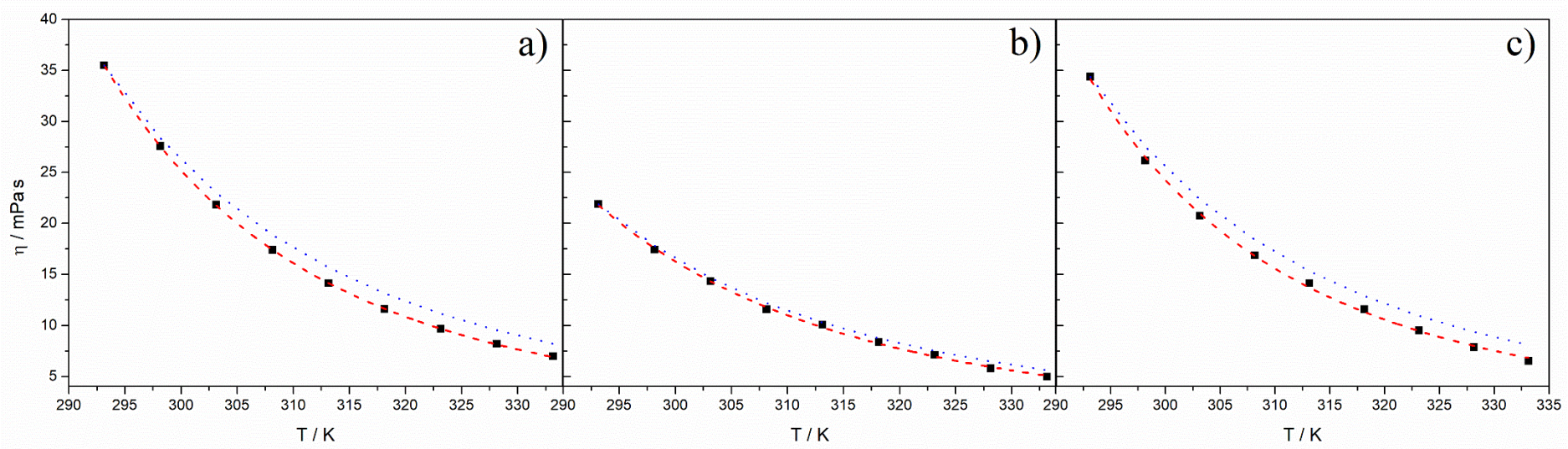

Figure 6 Experimental values of viscosities (black squares) for DES in the molar ratio 1:8 along with the predicted ones a) TBAB:MAE, b) TEAC:MAE, c) TBAC:MAE: red dashed line – VFT equation; blue dotted line – critical properties based method by Bakhtyari *et al.*.

Table 4 Fitting parameters for the Arrhenius equation for dynamic viscosity results determined within temperature range T = (293.15 to 333.15) K and P = 0.100 MPa.

DES	$10^5 \cdot \eta_\infty$ / mPa·s	$10^{-4} \cdot E_a$ / J·mol^{-1}	R^2	*RMSD*
DES1	1.70	3.60	0.9977	0.60
DES2	2.70	3.43	0.9989	0.33
DES3	2.54	3.42	0.9996	0.19
DES4	8.14	3.06	0.9984	0.25
DES5	9.67	3.00	0.9986	0.21
DES6	9.52	2.99	0.9994	0.13
DES7	1.46	3.64	0.9898	1.3
DES8	3.08	3.39	0.9977	0.44
DES9	8.42	3.11	0.9959	0.49

Table 5 Fitting parameters for the Vogel-Fulcher-Tamman (VFT) equation for dynamic viscosity results determined within temperature range T = (293.15 to 333.15) K and P = 0.100 MPa.

DES	η_0 / mPa·s	b / K	T_0 / K	R^2	*RMSD*
DES1	0.0706	727.5	180.6	0.9999	0.13
DES2	0.0213	1047.8	152.0	0.9999	0.05
DES3	0.0033	1672.1	111.2	0.9999	0.08
DES4	0.0430	836.1	160.7	0.9997	0.11
DES5	0.0065	1486.5	110.1	0.9988	0.20
DES6	0.0012	2196.6	67.2	0.9990	0.17
DES7	0.6784	269.7	229.6	0.9992	0.35
DES8	0.0344	904.3	162.1	0.9989	0.30
DES9	0.0686	750.3	169.3	0.9971	0.41

3.3.3 Refractive index

The refractive indices obtained for the DESs studied in this work are presented in Table S6. As can be seen, their values vary from 1.4541 to 1.4602 at the temperature of 298.15 K, which is consistent with the research conducted so far showing that the refractive indices of DESs are higher than molecular solvents such as ethanol or acetone, but similar to common ILs [52].

Regardless of the molar ratio of HBA to HBD, the refractive indices at a given temperature change according to: TBAB: MAE < TBAC: MAE < TEAC: MAE. Therefore, it

can be concluded that in the case of MAE-based DESs the main factor determining the refractive index values is molecular weight of solvent. Moreover, this observation is in agreement with the order of refractive indices obtained for DESs differing in the HBA:HBD molar ratio, because the n_D decrease with increasing MAE content for all DESs investigated.

Considering the decrease in refractive index with increasing temperature, it can be said that for MAE-based DESs, as with other published DESs based on alkanolamines such as monethanolamine, diethanolamine and 3-amino-1-propanol a linear decrease in refractive index with increasing temperature was observed [20][21][23]. This is presented in Fig. 7, which shows the obtained refractive indices for TBAB: MAE, TEAC: MAE and TBAB: MAE in the molar ratio 1:8 within the temperature range T = (293.15 to 333.15) K.

3.3.4 Speed of sound

The speed of sound data for the prepared MAE-based DESs measured at different temperatures are listed in Table S7 and presented in Figure 8.

As can be seen, the speed of sound decreases with increasing temperature. This is because sound waves travel slower in less-dense materials. Moreover, as with the density and refractive index, a linear relationship between the speed of sound and temperature is observed. Similar results were obtained by Omar and Sadeghi for deep eutectic solvents based on choline chloride [53].

At a given temperature and molar ratio of salt to 2-(methylamino)ethanol, the speed of sound changes in the order: TEAC:MAE > TBAC:MAE > TBAB:MAE, which is opposite with the order of refractive index. Thus, it can be concluded that the speed of sound of MAE-based DESs also depends mainly on the molecular weight of solvent, but unlike the refractive index it increases with its value.

Besides, the speed of sound of the DESs studied, similarly to other physical properties, also is related to the molar ratio of HBA to HBD. From Table S7 and Fig. 8 clearly is seen that for all deep eutectic solvents speed of sound decreases with increasing of molar ratio of MAE.

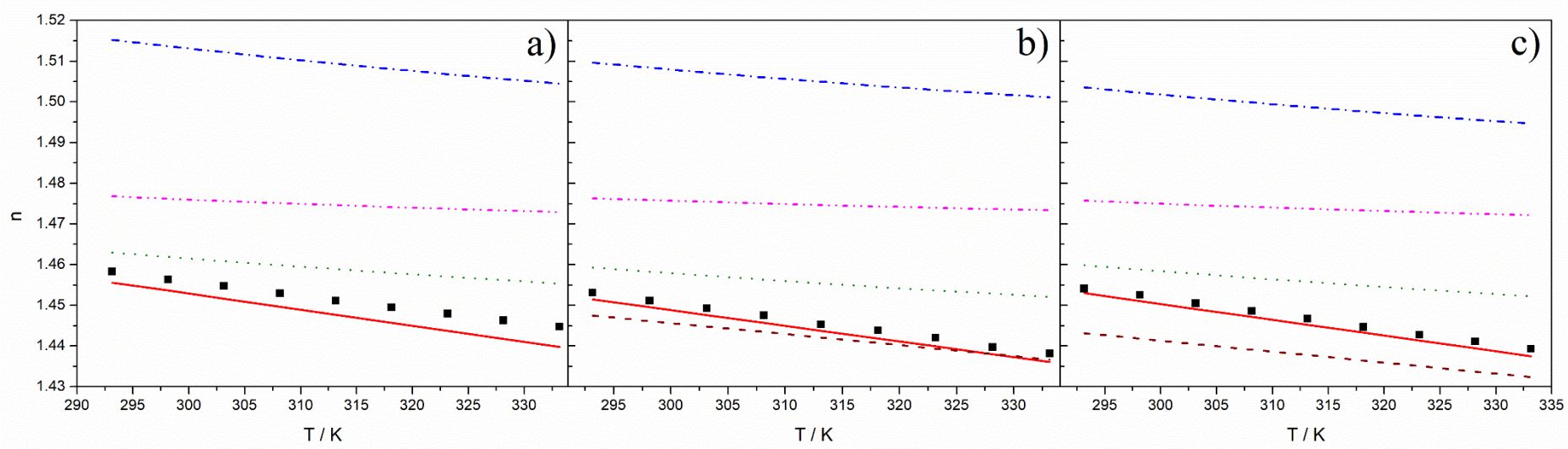

Figure 7 Experimental values of refractive indices (black squares) for DES in the molar ratio 1:8 a) TBAB:MAE, b) TEAC:MAE, c) TBAC:MAE along with predicted ones: red solid line – method based on molar refraction by Shabaz *et al*.; olive dotted line – method based on critical properties by Taherzadeh *et al.*; blue dashed-dotted line – GC based method by Haghbakhsh *et al.*; magenta dashed-dotted-dotted line – AC based method by Haghbakhsh *e. al.;* wine dashed line – GC based method by Khajeh *et al.*

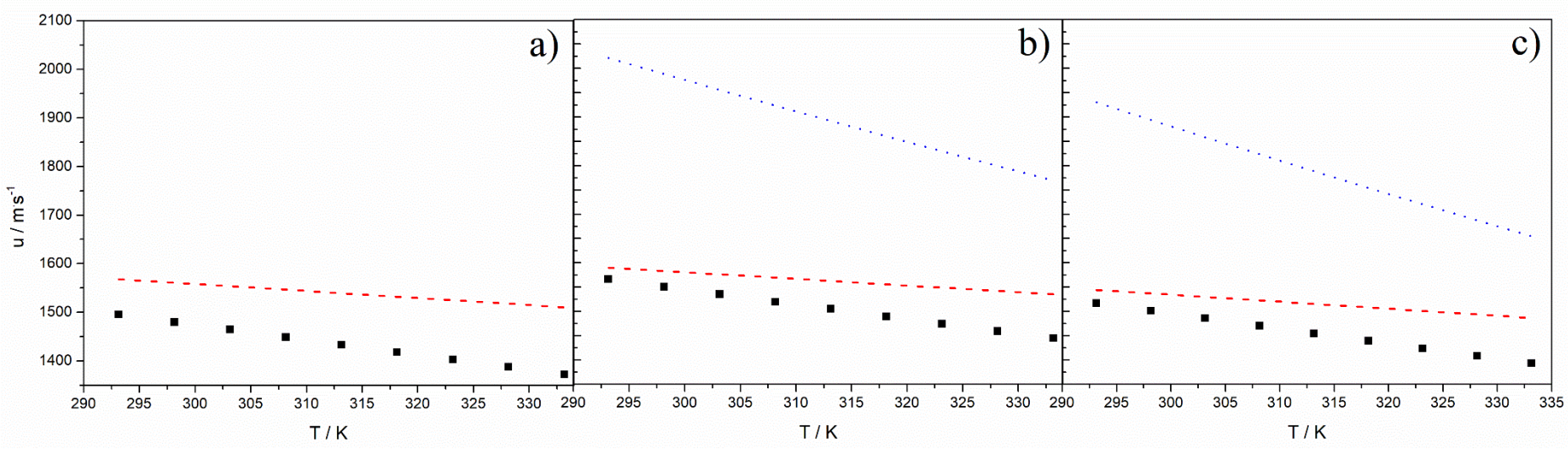

Figure 8 Experimental values of speed of sounds (black squares) for DES in the molar ratio 1:8 a) TBAB:MAE, b) TEAC:MAE, c) TBAC:MAE along with predicted ones: red dashed line – critical properties based method by Peyrovedin *et al.*; blue dotted line – AC based method by Haghbakhsh *et al.*.

3.4. Predicted values of physical properties of DESs

3.4.1 Density

For the DESs investigated in this study, the critical properties obtained with the Modified Lydersen-Joback-Reid method connected with the Lee-Kesler-mixing equations by Knapp *et al.* are presented in Table 6.

Table 6 Calculated mass connectivity indices, MCI, and critical properties of DESs used in this study: critical temperature, T_{cm}, critical volume, V_{cm}, critical pressure, P_{cm}, and acentric factor, ω.

DES	T_{cm} / K	V_{cm} / cm^3·mol^{-1}	P_{cm} / bar	ω	*MCI*
DES1	618.12	387.61	30.37	0.723	5.5607
DES2	611.23	365.27	31.94	0.717	6.7571
DES3	607.82	354.12	32.80	0.714	7.7272
DES4	589.93	334.65	34.18	0.674	4.8596
DES5	590.04	326.60	34.96	0.679	5.8900
DES6	590.14	321.24	35.51	0.683	6.9586
DES7	612.74	386.45	30.21	0.721	5.5758
DES8	607.39	365.39	31.74	0.716	6.6978
DES9	604.24	352.82	32.74	0.713	7.7715

Table 7 shows the obtained values of absolute average relative deviations (%AARD) between the experimental and predicted densities of the studied novel DESs based on 2-(methylamino)ethanol. The results for all seven methods, described in the paragraph 2, are also presented in Figure 5, which shows the experimental and modeled densities for DESs with the molar ratio 1:8. For solvents with the molar ratio of HBA to HBD equal to 1:6 and 1:10 similar relationships between the experimental and predicted values were obtained.

Results presented in Figure 5 reveals that the density values obtained by the models proposed by Haghbakhsh *et al.* (from both based on AC and critical properties) and Hou *et al.* are overestimated, while for the remaining models are underestimated. Moreover, our calculations indicate that all models, except those proposed by Haghbakhsh *et al.*, were able to capture the density variation correctly with increasing HBA:HBD molar ratio.

Table 7 Absolute average relative deviations (%AARD) for each model used for prediction of density values for DESs studied in this work.

DES	%AARD[1]	%AARD[2]	%AARD[3]	%AARD[4]	%AARD[5]	%AARD[6]	%AARD[7]
DES1	0.87	2.2	8.0	1.3	0.033	3.1	11
DES2	0.90	2.2	9.1	1.5	0.004	2.1	22
DES3	0.91	1.9	9.8	1.6	0.034	0.94	31
DES4	1.2	2.5	9.7	1.8	0.005	3.2	24
DES5	1.1	2.5	10	1.9	0.024	2.9	35
DES6	0.94	1.1	11	2.0	0.059	1.8	46
DES7	0.93	2.3	13	1.2	0.056	1.4	19
DES8	0.95	2.3	13	1.2	0.088	1.5	29
DES9	0.95	2.3	13	1.4	0.10	0.68	40

1- method based on Rackett equation by Spencer and Danner, 2- method based on Rackett equation by Mjalli, 3- method based on critical properties by Haghbakhsh *et al.* , 4- BGI based method, 5- MCI based method, 6-GC based method by Haghbakhsh *et al.*, 7- AC based method by Haghbakhsh *et al.*

The methods based on the Rackett equation by Spencer and Danner or by Mjalli and MCI based model have low %AARD values between 0.87% - 1.2%, 1.1% - 2.5% and 0.004% - 0.10%, respectively. Thus, these methods are characterized by a good prediction ability of the DESs studied so might be accepted and recommended for such purpose. However, it should remembered that all of them require knowledge of the experimental reference density data and the critical properties of DESs, which is a huge disadvantage. The BGI based model and the method based on GC proposed by Haghbakhsh *et al.* allow to obtain values of %AARD equal to 1.2% - 2.0% and 0.68% - 3.2%, respectively. Therefore, both models have good predicting ability, similar to the methods discussed above, but do not require any experimental data. The highest AARD% values are for the method based on critical properties and AC based model proposed by Haghbakhsh *et al.* (8.0% - 13% and 11% - 46%, respectively).

Summarizing the obtained AARD% results for all density prediction methods, it can be concluded that in the case of novel DESs based on MAE, if we do not have any experimental data, the best methods are the BGI model and the GC model proposed by Haghbakhsh *et al*. However, if we know the density value at one temperature at least, the best density values at other temperatures might be estimated using the MCI-based method.

3.4.2 Viscosity

Parameters *A* and *B* of the model for prediction of the viscosity proposed by Bakhtyari *et al.* [33] were calculated using the critical properties given in Table 6, and their values are presented in Table 8.

Table 8 Calculated values of *A* and *B* parameters DESs studied in this work.

DES	*A*	*B*
DES1	-0.14990	-985.91
DES2	-0.14858	-974.92
DES3	-0.14858	-974.92
DES4	-0.14690	-940.94
DES5	-0.14637	-941.12
DES6	-0.14601	-941.27
DES7	-0.15004	-977.33
DES8	-0.14874	-968.79
DES9	-0.14796	-963.76

Table 9 shows the obtained values of relative deviations (%RD) and absolute average relative deviations (%AARD) in temperature range 298.15 - 333.15 K. As it is presented, depending on DES, % AARD varies from 5.4% to 16%, which is close to the global % AARD value (10.1%) provided by the authors of this method [33]. Regardless of the temperature and composition of solvent, the predicted values were overestimated compared to the experimental ones, and the %RD increased with increasing temperature (see Figure 6). This observation suggests that this method has better viscosity predictive ability at temperatures close to the reference temperature. The relationship between the molar ratio of HBA to HBD and the viscosity of DESs was correctly modeled by the method. However, since the calculated values of % AARD exceed the viscosity measurement uncertainties found in practice, the model developed by Bakhtyari *et al.* does not appear to be suitable for an accurate estimation of MAE-based DESs viscosity. On the other side, as the predicted values maintain the viscosity order for TBAB:MAE, TEAC:MAE and TBAC:MAE, they can be used to select an appropriate DES from among the studied solvents for a specific application.

Table 9 Relative deviations (%RD) and absolute average relative deviation (%AARD) for model by Bakhtyari *et al.* for prediction of viscosity values for DESs studied in this work.

	DES1	DES2	DES3	DES4	DES5	DES6	DES7	DES8	DES9
T / K					*%RD*				
298.15	5.2	5.2	2.9	2.9	2.5	2.1	0.33	9.6	5.3
303.15	8.1	8.1	5.3	4.7	4.1	2.2	1.6	12	7.8
308.15	11	11	8.5	7.4	5.8	5.6	0.89	17	9.2
313.15	13	13	11	11	7.7	2.2	0.86	19	8.3
318.15	15	15	13	14	7.1	4.4	3.6	21	11
323.15	18	18	15	17	6.4	5.3	8.2	22	15
328.15	20	20	17	19	11	12	12	18	19
333.15	22	22	18.	23	12	13	16	10	24
%AARD	14	11	12	7.1	5.9	5.4	16	12	6.0

3.4.3 Refractive index

Table 10 shows the absolute average relative deviations (%AARD) for the calculated refractive indices in the temperature range 298.15 - 333.15 K. The results are also presented in Figure 5 including both the experimental and the predicted refractive indices for MAE-based DESs with the molar ratio 1:8. As can be seen, the predicted values calculated using the models proposed by Taherzadeh *et al.* and Haghbakhsh *et al.* are higher than the experimental values, while for other models they are lower. Moreover, our calculations showed that the models proposed by Shahbaz *et al.* and Taherzadeh *et al.* were able to predict a decrease of refractive index with an increase in the molar ratio of HBA to HBD, while others have not captured this relationship.

The best %AARD values (0.10% - 0.29%) were obtained using the model introduced by Shahbaz *et al.*. The major drawback of this method is that experimental density data is required to predict the refractive index.

The methods proposed by Taherzadeh *et al.* and Khajeh *et al.* are characterized by similar %AARD values (0.32% - 0.81% and 0.11% - 0.87% respectively), and the advantage of these models is that they do not require the use any of any experimental data, because they

are based solely on critical properties or group contribution. However, as written above, the method proposed by Khajeh *et al.* could not be used for alkanolamine-based DESs that contain TBAB.

The GC and AC models proposed by Haghbakhsh *et al.* have the highest %AARD values (2.8% - 4.7% and 1.3% - 2.2%, respectively), and therefore they are characterized by the worst refractive index prediction ability.

In summary, the most preferred model for prediction of refractive indices for novel MAE-based DESs is that introduced by Shahbaz *et al.,* but in the absence of experimental data on density, the method proposed by Taherzadeh *et al.* should be recommended.

Table 10 The %AARD of each model used for prediction of refractive index values for DESs studied in this work.

DES	%AARD[1]	%AARD[2]	%AARD[3]	%AARD[4]	%AARD[5]
DES1	0.29	0.32	-	3.2	1.3
DES2	0.25	0.53	-	4.0	1.6
DES3	0.22	0.67	-	4.7	1.8
DES4	0.18	0.46	0.49	3.4	1.8
DES5	0.12	0.69	0.24	4.1	2.0
DES6	0.13	0.81	0.11	4.7	2.2
DES7	0.16	0.42	0.87	2.8	1.6
DES8	0.10	0.64	0.61	3.6	1.9
DES9	0.13	0.75	0.48	4.2	2.0

1-method based on molar refraction by Shabaz *et al*., 2- method based on critical properties by Taherzadeh *et al.*, 3- GC based method by Khajeh *et al.*, 4- AC based method by Haghbakhsh *et al.*, 5- GC based method by Haghbakhsh *et al.*

3.4.4 Speed of sound

Figure 8 presents the correlation between the obtained experimental data and predicted speed of sound values for novel MAE-based DESs at a molar ratio 1:8. Similar relationships between the experimental and predicted values were obtained for these DESs with a molar ratio of HBA to HBD of 1:6 and 1:10. In Table 11, the absolute average relative deviations (%AARD) for calculated speed of sound of all mixtures in the temperature range 298.15 - 333.15 K are collected. Our calculations show that both models tends to overestimate the speed of sound for all DESs studied. Moreover, the method based on the critical properties and the method based on atomic contribution captured the negative variation of the speed of sound

values with temperature, but both failed to predict negative variability of *u* and MAE content. The %AARD of the first model ranges from 2.2% to 8.2%, while for the second model it is in the range of 20% - 29%. Thus, both models have a high %AARD, although the model introduced by Peyrovedin *et al.* is much better than the model proposed by Haghbakhsh *et al.*

Table 11 The %AARD of each model used for prediction of speed of sound values for novel DESs studied in this work.

DES	%AARD[1]	%AARD[2AC]
DES1	6.0	-
DES2	7.4	-
DES3	8.2	-
DES4	2.2	23
DES5	3.9	26
DES6	5.2	29
DES7	2.2	20
DES8	4.2	23
DES9	5.4	25

1-method based on critical properties by Peyrovedin *et al.*,

2-AC based method by Haghbakhsh *et al.*

4 Conclusions

In this work, experimental density, viscosity, refractive index and sound velocity for deep eutectic solvents based on 2-(methylamino)ethanol have been reported as a function of temperature at atmospheric pressure. Hydrogens bond acceptors in the studied DESs were tetrabutylammonium bromide, tetraethylammonium chloride and tetrabutylammonium chloride mixed with MAE in different molar ratios of 1:6, 1:8 and 1:10.

Spectroscopy measurements confirmed the hydrogen bonds interactions between components while thermal properties such as melting points and thermal stability of deep eutectic solvents are directly influenced by cation alkyl chain length in the salt. The results showed that for density, refractive index and speed of sound a linear negative correlation with temperature was obtained, while for viscosity the decrease with temperature was exponential.

The density of MAE-based DESs decreased with increasing chain length of HBD or HBA, but this effect was less than the effect of the anion weight. When the amount of alkanolamine in TBAB:MAE (DES 1-3) and TEAC:MAE (DES 4-6) increased, the density

decreased. For TBAC:MAE (DES 7-9), due to the similar density of DES and neat MAE, no significant changes in density were observed as a result of changing the solvent composition.

The lowest viscosity values for the studied systems were observed for TEAC-based DESs (DES4-6), which are smaller in size and where weaker hydrogen bonding is expected. Thus, in contrast to density, the alkyl chain length of the MAE-based DESs salts has a greater influence on the viscosity than the anion effect. Moreover, regardless of the salt, the viscosity decreased as the molar ratio of HBA to HBD increased.

The refractive indices of the studied DESs varied according to: TBAB:MAE < TBAC:MAE < TEAC: MAE and decreased with the decrease in salt content in the mixture. Thus, the main factor determining the refractive index of MAE-based DESs is their molecular weight. The speed of sound of TBAB:MAE, TEAC:MAE and TBAC:MAE also depends mainly on the molecular weight of the mixture, but unlike the refractive index it increases with its value. This is clearly seen both in the order of the speed of sound for DESs with different salts and for DESs with the same salts but a different molar ratio of HBA to HBD.

Moreover, models available in the literature were used and evaluated for prediction of the physicochemical properties of studied DESs. The results obtained in this work indicate that for deep eutectic solvents based on 2-(methylamino)ethanol, in the absence of any experimental data, the best models for density prediction are the bonding group interaction contribution method and the group contribution model. For modelling of refractive index, a method based on critical properties should be used. However, for viscosity or speed of sound, the methods using critical properties do not seem suitable for an accurate estimation of these properties for MAE-based DESs. The same effect, *i.e.* a higher % AARD value than the measurement uncertainties found in practice, was obtained for the atomic contribution method predicting the speed of sound of the DESs studied. Thus, the results indicate that new models that will be able to predict viscosity and speed of sound of alkanolamine-based DESs with lower %AARD are worth for searching.

FUNDING:

This research did not receive any specific grant from funding agencies in the public, commercial, or not-for-profit sectors.

References:

[1] K. Jafari, M. H. Fatemi, and P. Estellé, "Deep eutectic solvents (DESs): A short overview of the thermophysical properties and current use as base fluid for heat transfer nanofluids," *J. Mol. Liq.*, vol. 321, 2021, doi: 10.1016/j.molliq.2020.114752.

[2] B. B. Hansen *et al.*, "Deep Eutectic Solvents: A Review of Fundamentals and Applications," *Chem. Rev.*, vol. 121, no. 3, pp. 1232–1285, 2021, doi: 10.1021/acs.chemrev.0c00385.

[3] I. Wazeer, M. Hayyan, and M. K. Hadj-Kali, "Deep eutectic solvents: designer fluids for chemical processes," *J. Chem. Technol. Biotechnol.*, vol. 93, no. 4, pp. 945–958, 2018, doi: 10.1002/jctb.5491.

[4] Y. Marcus, *Deep Eutectic Solvents*. Springer International Publishing, 2019.

[5] E. Gómez, P. Cojocaru, L. Magagnin, and E. Valles, "Electrodeposition of Co, Sm and SmCo from a Deep Eutectic Solvent," *J. Electroanal. Chem.*, vol. 658, no. 1–2, pp. 18–24, 2011, doi: 10.1016/j.jelechem.2011.04.015.

[6] Q. Zhang, K. De Oliveira Vigier, S. Royer, and F. Jérôme, "Deep eutectic solvents: Syntheses, properties and applications," *Chem. Soc. Rev.*, vol. 41, no. 21, pp. 7108–7146, 2012, doi: 10.1039/c2cs35178a.

[7] M. Pätzold, S. Siebenhaller, S. Kara, A. Liese, C. Syldatk, and D. Holtmann, "Deep Eutectic Solvents as Efficient Solvents in Biocatalysis," *Trends Biotechnol.*, vol. 37, no. 9, pp. 943–959, 2019, doi: 10.1016/j.tibtech.2019.03.007.

[8] F. S. Oliveira, A. B. Pereiro, L. P. N. Rebelo, and I. M. Marrucho, "Deep eutectic solvents as extraction media for azeotropic mixtures," *Green Chem.*, vol. 15, no. 5, pp. 1326–1330, 2013, doi: 10.1039/c3gc37030e.

[9] S. Sarmad, J. P. Mikkola, and X. Ji, "Carbon Dioxide Capture with Ionic Liquids and Deep Eutectic Solvents: A New Generation of Sorbents," *ChemSusChem*, vol. 10, no. 2, pp. 324–352, 2017, doi: 10.1002/cssc.201600987.

[10] M. Mokhtarpour, H. Shekaari, M. T. Zafarani-Moattar, and S. Golgoun, "Solubility and solvation behavior of some drugs in choline based deep eutectic solvents at different temperatures," *J. Mol. Liq.*, vol. 297, 2020, doi: 10.1016/j.molliq.2019.111799.

[11] M. Zhang *et al.*, "Insights into the relationships between physicochemical properties, solvent performance, and applications of deep eutectic solvents," *Environ. Sci. Pollut. Res.*, vol. 28, no. 27, pp. 35537–35563, 2021, doi: 10.1007/s11356-021-14485-2.

[12] R. Haghbakhsh, S. Raeissi, and A. R. C. Duarte, "Group contribution and atomic contribution models for the prediction of various physical properties of deep eutectic

solvents," *Sci. Rep.*, vol. 11, no. 1, 2021, doi: 10.1038/s41598-021-85824-z.

[13] K. Shahbaz, F. S. G. Bagh, F. S. Mjalli, I. M. AlNashef, and M. A. Hashim, "Prediction of refractive index and density of deep eutectic solvents using atomic contributions," *Fluid Phase Equilib.*, vol. 354, pp. 304–311, Sep. 2013, doi: 10.1016/j.fluid.2013.06.050.

[14] K. Shahbaz, F. S. Mjalli, M. A. Hashim, and I. M. Alnashef, "Prediction of deep eutectic solvents densities at different temperatures," *Thermochim. Acta*, vol. 515, no. 1–2, pp. 67–72, 2011, doi: 10.1016/j.tca.2010.12.022.

[15] N. R. Mirza, N. J. Nicholas, Y. Wu, S. Kentish, and G. W. Stevens, "Estimation of Normal Boiling Temperatures, Critical Properties, and Acentric Factors of Deep Eutectic Solvents," *J. Chem. Eng. Data*, vol. 60, no. 6, pp. 1844–1854, 2015, doi: 10.1021/acs.jced.5b00046.

[16] H. Peyrovedin, R. Haghbakhsh, A. R. C. Duarte, and S. Raeissi, "A Global Model for the Estimation of Speeds of Sound in Deep Eutectic Solvents," *Molecules*, vol. 25, no. 7, p. 1626, Apr. 2020, doi: 10.3390/molecules25071626.

[17] K. Shahbaz, S. Baroutian, F. S. Mjalli, M. A. Hashim, and I. M. Alnashef, "Densities of ammonium and phosphonium based deep eutectic solvents: Prediction using artificial intelligence and group contribution techniques," *Thermochim. Acta*, vol. 527, pp. 59–66, 2012, doi: 10.1016/j.tca.2011.10.010.

[18] A. Khajeh, K. Parvaneh, and M. Shakourian-Fard, "Refractive index prediction of deep eutectic solvents by molecular approaches," *J. Mol. Liq.*, vol. 332, p. 115843, Jun. 2021, doi: 10.1016/j.molliq.2021.115843.

[19] Z. Li *et al.*, "Absorption of Carbon Dioxide Using Ethanolamine-Based Deep Eutectic Solvents," *ACS Sustain. Chem. Eng.*, vol. 7, no. 12, pp. 10403–10414, 2019, doi: 10.1021/acssuschemeng.9b00555.

[20] F. S. Mjalli, G. Murshid, S. Al-Zakwani, and A. Hayyan, "Monoethanolamine-based deep eutectic solvents, their synthesis and characterization," *Fluid Phase Equilib.*, vol. 448, pp. 30–40, 2017, doi: 10.1016/j.fluid.2017.03.008.

[21] G. Murshid, F. S. Mjalli, J. Naser, S. Al-Zakwani, and A. Hayyan, "Novel diethanolamine based deep eutectic mixtures for carbon dioxide (CO 2) capture: synthesis and characterisation," *Phys. Chem. Liq.*, vol. 57, no. 4, pp. 473–490, 2019, doi: 10.1080/00319104.2018.1491043.

[22] I. Adeyemi, M. R. M. Abu-Zahra, and I. M. AlNashef, "Physicochemical properties of alkanolamine-choline chloride deep eutectic solvents: Measurements, group

contribution and artificial intelligence prediction techniques," *J. Mol. Liq.*, vol. 256, pp. 581–590, 2018, doi: 10.1016/j.molliq.2018.02.085.

[23] B. Nowosielski, M. Jamrógiewicz, J. Łuczak, M. Śmiechowski, and D. Warmińska, "Experimental and predicted physicochemical properties of monopropanolamine-based deep eutectic solvents," *J. Mol. Liq.*, vol. 309, 2020, doi: 10.1016/j.molliq.2020.113110.

[24] H. G. Rackett, "Equation of State for Saturated Liquids," *J. Chem. Eng. Data*, vol. 15, no. 4, pp. 514–517, 1970, doi: 10.1021/je60047a012.

[25] C. F. Spencer and R. P. Danner, "Improved Equation for Prediction of Saturated Liquid Density," *J. Chem. Eng. Data*, vol. 17, no. 2, pp. 236–241, 1972, doi: 10.1021/je60053a012.

[26] F. S. Mjalli, K. Shahbaz, and I. M. AlNashef, "Modified Rackett equation for modelling the molar volume of deep eutectic solvents," *Thermochim. Acta*, vol. 614, pp. 185–190, Aug. 2015, doi: 10.1016/j.tca.2015.06.026.

[27] V. H. Alvarez and J. O. Valderrama, "A modified Lydersen-Joback-Reid method to estimate the critical properties of biomolecules," *Alimentaria*, vol. 254, pp. 55–66, 2004.

[28] H. Knapp, R. Doring, L. Oellrich, U. Plocker, and J. M. Prausnitz, "Vapor-Liquid Equilibria for Mixtures of Low Boiling Substances, Chemistry Data Series, vol. VI," *VI (DECHEMA, Frankfurt, Ger. 1982)*, 1982.

[29] R. Haghbakhsh, R. Bardool, A. Bakhtyari, A. R. C. Duarte, and S. Raeissi, "Simple and global correlation for the densities of deep eutectic solvents," *J. Mol. Liq.*, vol. 296, p. 111830, Dec. 2019, doi: 10.1016/j.molliq.2019.111830.

[30] X.-J. Hou, L.-Y. Yu, Y.-X. Wang, K.-J. Wu, and C.-H. He, "Comprehensive Prediction of Densities for Deep Eutectic Solvents: A New Bonding-Group Interaction Contribution Scheme," *Ind. Eng. Chem. Res.*, vol. 60, no. 35, pp. 13127–13139, Sep. 2021, doi: 10.1021/acs.iecr.1c02260.

[31] F. S. Mjalli, "Mass connectivity index-based density prediction of deep eutectic solvents," *Fluid Phase Equilib.*, vol. 409, pp. 312–317, 2016, doi: 10.1016/j.fluid.2015.09.053.

[32] J. O. Valderrama and R. E. Rojas, "Mass connectivity index, a new molecular parameter for the estimation of ionic liquid properties," *Fluid Phase Equilib.*, vol. 297, no. 1, pp. 107–112, 2010, doi: 10.1016/j.fluid.2010.06.015.

[33] A. Bakhtyari, R. Haghbakhsh, A. R. C. Duarte, and S. Raeissi, "A simple model for the

viscosities of deep eutectic solvents," *Fluid Phase Equilib.*, vol. 521, p. 112662, Oct. 2020, doi: 10.1016/j.fluid.2020.112662.

[34] S. A. Wildman and G. M. Crippen, "Prediction of Physicochemical Parameters by Atomic Contributions," *J. Chem. Inf. Comput. Sci.*, vol. 39, no. 5, pp. 868–873, Sep. 1999, doi: 10.1021/ci990307l.

[35] M. Taherzadeh, R. Haghbakhsh, A. R. C. Duarte, and S. Raeissi, "Generalized Model to Estimate the Refractive Indices of Deep Eutectic Solvents," *J. Chem. Eng. Data*, vol. 65, no. 8, pp. 3965–3976, 2020, doi: 10.1021/acs.jced.0c00308.

[36] I. Zahrina, K. Mulia, A. Yanuar, and M. Nasikin, "Molecular interactions in the betaine monohydrate-polyol deep eutectic solvents: Experimental and computational studies," *J. Mol. Struct.*, vol. 1158, pp. 133–138, 2018, doi: 10.1016/j.molstruc.2017.11.064.

[37] H. Ghaedi, M. Ayoub, S. Sufian, B. Lal, and Y. Uemura, "Thermal stability and FT-IR analysis of Phosphonium-based deep eutectic solvents with different hydrogen bond donors," *J. Mol. Liq.*, vol. 242, pp. 395–403, 2017, doi: 10.1016/j.molliq.2017.07.016.

[38] E. L. Smith, A. P. Abbott, and K. S. Ryder, "Deep Eutectic Solvents (DESs) and Their Applications," *Chem. Rev.*, vol. 114, no. 21, pp. 11060–11082, 2014, doi: 10.1021/cr300162p.

[39] C. Florindo, F. S. Oliveira, L. P. N. Rebelo, A. M. Fernandes, and I. M. Marrucho, "Insights into the synthesis and properties of deep eutectic solvents based on cholinium chloride and carboxylic acids," *ACS Sustain. Chem. Eng.*, vol. 2, no. 10, pp. 2416–2425, 2014, doi: 10.1021/sc500439w.

[40] Y. Wang, Y. Hou, W. Wu, D. Liu, Y. Ji, and S. Ren, "Roles of a hydrogen bond donor and a hydrogen bond acceptor in the extraction of toluene from: N -heptane using deep eutectic solvents," *Green Chem.*, vol. 18, no. 10, pp. 3089–3097, 2016, doi: 10.1039/c5gc02909k.

[41] H. Ghaedi, M. Ayoub, S. Sufian, B. Lal, and A. M. Shariff, "Measurement and correlation of physicochemical properties of phosphonium-based deep eutectic solvents at several temperatures (293.15 K–343.15 K) for CO2 capture," *J. Chem. Thermodyn.*, vol. 113, pp. 41–51, 2017, doi: 10.1016/j.jct.2017.05.020.

[42] A. P. Abbott, R. C. Harris, K. S. Ryder, C. D'Agostino, L. F. Gladden, and M. D. Mantle, "Glycerol eutectics as sustainable solvent systems," *Green Chem.*, vol. 13, no. 1, pp. 82–90, 2011, doi: 10.1039/c0gc00395f.

[43] S. Sarmad, Y. Xie, J. P. Mikkola, and X. Ji, "Screening of deep eutectic solvents (DESs) as green CO2 sorbents: from solubility to viscosity," *New J. Chem.*, vol. 41, no.

1, pp. 290–301, 2016, doi: 10.1039/c6nj03140d.

[44] R. Saputra, R. Walvekar, M. Khalid, and N. M. Mubarak, “Synthesis and thermophysical properties of ethylammonium chloride-glycerol-ZnCl2 ternary deep eutectic solvent,” *J. Mol. Liq.*, vol. 310, p. 113232, Jul. 2020, doi: 10.1016/j.molliq.2020.113232.

[45] N. Rodriguez Rodriguez, L. Machiels, and K. Binnemans, “p -Toluenesulfonic Acid-Based Deep-Eutectic Solvents for Solubilizing Metal Oxides,” *ACS Sustain. Chem. Eng.*, vol. 7, no. 4, pp. 3940–3948, Feb. 2019, doi: 10.1021/acssuschemeng.8b05072.

[46] A. P. Abbott, G. Capper, and S. Gray, “Design of Improved Deep Eutectic Solvents Using Hole Theory,” *ChemPhysChem*, vol. 7, no. 4, pp. 803–806, Apr. 2006, doi: 10.1002/cphc.200500489.

[47] T. El Achkar, H. Greige-Gerges, and S. Fourmentin, “Basics and properties of deep eutectic solvents: a review,” *Environ. Chem. Lett.*, vol. 19, no. 4, pp. 3397–3408, 2021, doi: 10.1007/s10311-021-01225-8.

[48] A. P. Abbott, R. C. Harris, and K. S. Ryder, “Application of hole theory to define ionic liquids by their transport properties,” *J. Phys. Chem. B*, vol. 111, no. 18, pp. 4910–4913, 2007, doi: 10.1021/jp0671998.

[49] M. Francisco, A. van den Bruinhorst, and M. C. Kroon, “Low-Transition-Temperature Mixtures (LTTMs): A New Generation of Designer Solvents,” *Angew. Chemie Int. Ed.*, vol. 52, no. 11, pp. 3074–3085, Mar. 2013, doi: 10.1002/anie.201207548.

[50] A. Hayyan, F. S. Mjalli, I. M. Alnashef, Y. M. Al-Wahaibi, T. Al-Wahaibi, and M. A. Hashim, “Glucose-based deep eutectic solvents: Physical properties,” *J. Mol. Liq.*, vol. 178, pp. 137–141, 2013, doi: 10.1016/j.molliq.2012.11.025.

[51] S. P. Ijardar, V. Singh, and R. L. Gardas, “Revisiting the Physicochemical Properties and Applications of Deep Eutectic Solvents,” *Molecules*, vol. 27, no. 4, p. 1368, Feb. 2022, doi: 10.3390/molecules27041368.

[52] S. Seki *et al.*, “Comprehensive refractive index property for room-temperature ionic liquids,” *J. Chem. Eng. Data*, vol. 57, no. 8, pp. 2211–2216, 2012, doi: 10.1021/je201289w.

[53] K. A. Omar and R. Sadeghi, “Novel Nonanol-Based deep eutectic solvents: Thermophysical properties and their applications in Liquid-Liquid extraction and amino acid detection,” *J. Mol. Liq.*, vol. 336, 2021, doi: 10.1016/j.molliq.2021.116359.

Effect of temperature and composition on physical properties of deep eutectic solvents based on 2-(methylamino)ethanol – measurement and prediction

Bartosz Nowosielski[a], Marzena Jamrógiewicz[b], Justyna Łuczak[c, d], Agnieszka Tercjak[e], Dorota Warmińska[a, *]

[a] Department of Physical Chemistry, Faculty of Chemistry, Gdańsk University of Technology, ul. Narutowicza 11/12, 80-233 Gdańsk, POLAND

[b] Department of Physical Chemistry, Faculty of Pharmacy, Medical University of Gdańsk, Al. Gen. Hallera 107, 80-416 Gdańsk, POLAND

[c] Department of Process Engineering and Chemical Technology, Faculty of Chemistry, Gdańsk University of Technology, ul. Narutowicza 11/12, 80-233 Gdańsk, POLAND

[d] Advanced Materials Center, Gdańsk University of Technology, ul. Narutowicza 11/12, 80–233 Gdańsk, POLAND[c] Department of Physical Chemistry, Faculty of Pharmacy, Medical University of Gdańsk, Al. Gen. Hallera 107, 80-416 Gdańsk, POLAND

[e] Group 'Materials + Technologies' (GMT), Department of Chemical and Environmental Engineering, Faculty of Engineering, University of the Basque Country (UPV/EHU), Pza Europa 1, 20018 Donostia-San Sebastian, Spain

[*]Corresponding author: Tel.:+48583471410; fax:+48583472694,
e-mail address: dorwarmi@ pg.edu.pl

Table S1 Parameters of model proposed by Haghbakhsh *et. al.* [1].

parameter	values
A_1	-0.00000113
A_2	0.002566
A_3	0.2376
A_4	-0.000467
B	-0.000464

Table S2 Parameters of model proposed by Hou *et.al.* [2].

parameter	values
A1	3.8043
A2	1.0601
B1	0.000382
B2	-0.000672
G_{III}	0.0000342

Table S3 Parameters of model proposed by Taherzadeh *et al.* [3].

parameters	values
A_1	0.0517
A_2	-11.625
A_3	0.00227
A_4	1.3668
B	25.89

Table S4 Experimental density, d, of deep eutectic solvents within temperature range T = (293.15 to 333.15) K and P = 0.100 MPa[a] .

T / K	DES1	DES2	DES3	DES4	DES5	DES6	DES7	DES8	DES9
				d / (kg·m^{-3})					
293.15	986.1	978.0	973.3	958.9	956.0	953.8	939.6	940.3	940.0
298.15	982.4	974.4	969.6	955.5	952.4	950.2	936.2	936.8	936.4
303.15	978.8	970.7	965.9	952.0	948.9	946.7	932.8	933.3	932.9
308.15	975.2	967.0	962.2	948.5	945.3	943.1	929.3	929.9	929.3
313.15	971.5	963.3	958.5	945.0	941.8	939.5	925.9	926.4	925.7
318.15	967.8	959.6	954.8	941.5	938.2	935.9	922.5	922.9	922.2
323.15	964.3	955.9	951.1	938.1	934.7	932.3	919.1	919.4	918.6
328.15	960.7	952.2	947.3	934.6	931.1	928.7	915.6	915.9	915.0
333.15	957.1	948.5	943.6	931.1	927.6	923.0	912.2	912.4	911.4

[a] Standard uncertainties u are $u(T)$ =0.01 K, $u(p)$= 0.001 MPa, $u(d)$ = 0.1 kg·m^{-3}

Table S5 Experimental viscosities, η, of deep eutectic solvents within temperature range T = (293.15 to 333.15) K and P = 0.100 MPa[a].

T / K	DES1	DES2	DES3	DES4	DES5	DES6	DES7	DES8	DES9
				η / (mPa·s)					
293.15	45.27	35.51	32.55	23.70	21.89	20.50	47.35	34.37	29.49
298.15	34.12	27.57	25.32	18.78	17.43	16.74	34.27	26.15	22.94
303.15	26.71	21.82	20.21	15.20	14.33	13.53	27.02	20.75	18.46
308.15	21.15	17.38	16.21	12.45	11.55	11.36	21.09	16.84	15.12
313.15	17.14	14.13	13.09	10.28	10.05	9.57	17.15	14.13	12.73
318.15	14.07	11.59	10.63	8.78	8.35	7.92	14.07	11.56	11.44
323.15	11.64	9.64	8.82	7.56	7.10	6.50	11.78	9.50	8.93
328.15	9.73	8.16	7.42	6.23	5.78	5.45	10.35	7.84	7.38
333.15	8.17	6.95	6.21	5.41	4.95	4.57	9.58	6.50	6.48

[a] Standard uncertainties u are $u(T)$ =0.01 K, $u(p)$= 0.001 MPa, $u(\eta)$ = 2%

Table S6 Experimental refractive indices, $n_{D,}$ of deep eutectic solvents within temperature range T = (293.15 to 333.15) K and P = 0.100 MPa[a].

T / K	DES1	DES2	DES3	DES4	DES5	DES6	DES7	DES8	DES9
				n_D					
293.15	1.4618	1.4583	1.4560	1.4560	1.4531	1.4510	1.4571	1.4541	1.4520
298.15	1.4602	1.4563	1.4541	1.4542	1.4511	1.4489	1.4551	1.4525	1.4504
303.15	1.4587	1.4547	1.4524	1.4526	1.4492	1.4472	1.4536	1.4505	1.4482
308.15	1.4570	1.4529	1.4504	1.4509	1.4475	1.4454	1.4519	1.4486	1.4466
313.15	1.4552	1.4511	1.4487	1.4490	1.4453	1.4437	1.4502	1.4467	1.4449
318.15	1.4537	1.4495	1.4469	1.4474	1.4438	1.4418	1.4486	1.4446	1.443
323.15	1.4519	1.4479	1.4450	1.4455	1.442	1.4399	1.4469	1.4427	1.4411
328.15	1.4505	1.4463	1.4434	1.4439	1.4397	1.4382	1.4452	1.4411	1.4392
333.15	1.4491	1.4447	1.4417	1.4424	1.4381	1.4366	1.4439	1.4393	1.4377

[a] Standard uncertainties u are $u(T)$ =0.1 K, $u(p)$= 0.001 MPa, $u(n_D)$ = 0.0002

Table S7 Experimental speed of sound values, $u,$ for DESs within temperature range T = (293.15 to 333.15) K and P = 0.100 MPa[a].

T / K	DES1	DES2	DES3	DES4	DES5	DES6	DES7	DES8	DES9
				u / m·s^{-1}					
293.15	1497.5	1495.2	1494.1	1581.2	1565.5	1553.4	1521.4	1516.6	1513.3
298.15	1482.0	1479.7	1478.5	1565.6	1550.1	1538.0	1505.8	1501.0	1497.6
303.15	1466.6	1464.1	1462.9	1550.1	1534.8	1522.5	1490.2	1485.3	1482.0
308.15	1451.3	1448.7	1447.5	1534.7	1519.5	1507.1	1474.7	1469.8	1466.3
313.15	1435.8	1433.1	1431.9	1519.3	1504.6	1491.9	1459.1	1454.2	1450.5
318.15	1420.7	1417.8	1416.5	1504.3	1489.4	1476.9	1443.8	1438.9	1435.0
323.15	1405.5	1402.6	1401.2	1489.1	1474.1	1461.5	1428.6	1423.6	1419.5
328.15	1390.5	1387.3	1385.9	1473.8	1458.8	1446.3	1413.5	1408.3	1404.1
333.15	1375.4	1372.2	1370.6	1458.7	1444.6	1431.0	1398.5	1393.1	1388.5

[a] Standard uncertainties u are $u(T)$ =0.01 K, $u(p)$= 0.001 MPa, $u(u)$ = 0.5 m·s^{-1}

[1] R. Haghbakhsh, R. Bardool, A. Bakhtyari, A. R. C. Duarte, and S. Raeissi, “Simple and global correlation for the densities of deep eutectic solvents,” *J. Mol. Liq.*, vol. 296, p. 111830, Dec. 2019, doi: 10.1016/j.molliq.2019.111830.

[2] X.-J. Hou, L.-Y. Yu, Y.-X. Wang, K.-J. Wu, and C.-H. He, “Comprehensive Prediction of Densities for Deep Eutectic Solvents: A New Bonding-Group Interaction Contribution Scheme,” *Ind. Eng. Chem. Res.*, vol. 60, no. 35, pp. 13127–13139, Sep. 2021, doi: 10.1021/acs.iecr.1c02260.

[3] M. Taherzadeh, R. Haghbakhsh, A. R. C. Duarte, and S. Raeissi, “Generalized Model to Estimate the Refractive Indices of Deep Eutectic Solvents,” *J. Chem. Eng. Data*, vol. 65, no. 8, pp. 3965–3976, Aug. 2020, doi: 10.1021/acs.jced.0c00308.